ALCHEMY Jurnal Penelitian Kimia

Official Website: https://jurnal.uns.ac.id/alchemy

ISSN 1412-4092
EISSN 2443-4183

Review

Phloroglucinol Compounds and Their Derivatives: Comparison of FTIR, NMR, and Bioactivity Characterization as Antibacterial, Antioxidant, and Anticancer Agents

Sevi Dwi Cahyani[a], Triana Kusumaningsih[a, b*], Maulidan Firdaus[a], Wahyu Eko Prasetyo[c]

[a]*Master Program of Chemistry, Faculty of Mathematics and Natural Sciences, Sebelas Maret University*
Jl. Ir. Sutami 36 A, Kentingan, Surakarta, 57126, Indonesia
[b]*Halal Research Center and Services, Sebelas Maret University, Surakarta, Indonesia*
Jl. Ir. Sutami 36 A, Kentingan, Surakarta, 57126, Indonesia
[c]*College of Pharmacy and Research Institute of Drug Development, Chonnam National University*
Gwangju 61186, Korea

[*]*Corresponding author: triana_kusumaningsih@staff.uns.ac.id*

DOI:10.20961/alchemy.22.1.109425.1-39

Received 6 October 2025, Revised 22 December 2025, Accepted 29 December 2025, Published 31 March 2026

Keywords:

antibacterial; anticancer; antioxidant; phloroglucinol; phloroglucinol derivatives.

ABSTRACT. Research on phloroglucinol (PG) and its derivatives has been extensively pursued over the past three decades. PG compounds are found in many plants, such as in the genus *Callopyillum,* the genus *Hypericum, Eucalyptus kino*, and brown algae. PG compounds have a symmetrical compound structure and contain many electrons distributed across three active sites, making them very advantageous for electrophilic aromatic substitution. PG has biological activities, such as antibacterial, antioxidant, anticancer, antiviral, anti-inflammatory, and others. PG bioactivity can be increased by synthesizing PG derivatives using various synthetic methods. The addition of an active group to PG can affect its bioactivity, properties, and characteristics, as well as its polarity and lipophilicity. This study aims to collect data on (1) Comparison of Fourier transform infrared (FTIR) and nuclear magnetic resonance (NMR) characterization of various PG derivative compounds, (2) Comparison of PG bioactivity and its derivatives as antibacterial, antioxidant, and anticancer compounds. PG compounds and their derivatives have been shown to exhibit antibacterial effects against several bacteria, including Staphylococcus aureus, Escherichia coli, and MRSA. Furthermore, PG derivatives exhibit antioxidant properties, as evidenced by their low IC_{50} values, and have demonstrated anticancer activity against cancer cell lines such as A549, MCF-7, and HTC-116. The findings of this study have the potential to assist researchers in developing new drugs.

CONTENTS

INTRODUCTION

Phloroglucinol or 1,3,5-trihydroxybenzene (PG) is widely found in the genus *Callopylum*, genus *Hypericum,* and brown algae class (Biessy and Filion, 2021), *Eucalyptus corpo, Acacia arabica,* and marine algae family Phaeophyceae and Fucaceae (Singh and Bharate, 2006). In Indonesia, *Calophyllum inophyllum* Lin is known as the nyamplung plant, and all parts of the plant are used to treat various diseases, which are widespread in North Sumatra, Nusa Tenggara, Bali, and Sulawesi (Apparatus *et al.*, 2018). In the pharmaceutical field, this plant has been reported to exhibit various biological activities, namely antibacterial, anticancer, anti-inflammatory, and antiviral. Genus *Calophyllum* is identified as rich in phenolic compounds, including flavonoids, xanthone, coumarin, terpenoids, carboxylic chloranonic acid, and PG (Aminudin *et al.,* 2019). Phenolic compounds are

Cite this as: Cahyani, S. D., Kusumaningsih, T., Firdaus, M., and Prasetyo, W. E. (2026). Phloroglucinol Compounds and Their Derivatives: Comparison of FTIR, NMR, and Bioactivity Characterization as Antibacterial, Antioxidant, and Anticancer Agents. *ALCHEMY Jurnal Penelitian Kimia*, 22(1), 1-39. doi: https://dx.doi.org/10.20961/alchemy.22.1.109425.1-39.

compounds that have an aromatic ring structure with one or more hydroxyl groups (Diniyah and Lee, 2020). This compound is produced for protection against UV rays, viruses, bacteria, and insects (Greece *et al.*, 2015). Natural phenolic compounds are currently widely used in the pharmaceutical field due to their broad applications and many bioactivities (Stuttgart *et al*., 2019).

PG compounds have a wide range of uses, including medicine, dyes, cosmetics, pesticides, and paints (Singh *et al.*, 2009). About 700 PG-based natural products have been reported to exhibit a wide range of biological activities (Prasetyo *et al.*, 2022). Bioactivity of PG compounds, such as antibacterial, antioxidant, anti-allergic, anti-inflammatory, anti-insect (Mondal *et al.,* 2017), anticancer (Kusumaningsih *et al.,* 2023), antifungal (Prasetyo *et al*., 2022), and antiplasmodial (Hertiningtyas *et al.,* 2013). In modern pharmacological research, PG compounds in fern-type plants have been shown to exhibit strong bactericidal, antiviral, and insect-repellent effects (Yang *et al.,* 2024). Bridi *et al.* (2018) reported that many studies on PG derivatives account for most of the biological activity, suggesting that PG has high potential as a new drug candidate.

The combination of PG compounds with other compounds to obtain new compounds that can improve their bioactivity, properties, and characteristics has been widely pursued by researchers. One of them is to make modifications and/or add new clusters. PG derivative products can be in the form of phloroglucinol derivatives, phloroglucinol dimers, phloroglucinol trimers, terpene phloroglucinol, phloroglucinol glycosides, phloroglucinol halogens, and others (Kusumaningsih *et al.,* 2016). One of the derivative products of PG that is most promising in increasing bioactivity is the result of phloroglucinol (APG) (Prasetyo *et al*., 2022). Examples of widely used groups in PG modification are acetyl acetate, isobutyryl, and isovaleryl (Prasetyo *et al*., 2023), as well as formaldehyde, propionyl, and butyryl (Yang *et al*., 2024). APG compounds are a class of PG derivatives with many biological activities. Derivative compounds, such as monoacyl phloroglucinol and diacyl phloroglucinol, have shown potential as antibacterial, antioxidant, anti-allergic pharmacological agents, enzyme inhibitors, antidepressants, anti-inflammatory agents, and antitumor agents (Kusumaningsih *et al*., 2019; Li *et al*., 2009).

PG compounds are well known for their various biological activities. APG compounds exhibit significant antibacterial activity against several Gram-positive bacteria, including Methicillin-r*esistant Staphylococcus aureus* (MRSA) (Morkunas *et al.*, 2013). In addition, APG has strong antibacterial activity against *Staphylococcus aureus (S. aureus)* and *Mycobacterium smegmatis* (Henry *et al*., 2008). Bridi *et al.* (2018) reported that APG dimer compounds exhibit antibacterial activity against S. aureus, *Bacillus subtilis* (B. subtilis), and *Mycobacterium smegmatis*, with inhibitory values of <7 µg/mL. *S. aureus* is one of the gram-positive pathogens that is a serious threat to world health, causing various kinds of infectious diseases such as skin infections, bacteremia, meningitis, endocarditis, and others (Prasetyo *et al*., 2023). In addition to antibacterial activity, this compound also has antioxidant activity. APG compounds have aromatic substituents that confer high antioxidant activity (Sun *et al*., 2014). Prasetyo *et al*. (2022) reported that APG compounds exhibit high antioxidant activity, with IC_{50} values of 10 – 50 mg/mL.

Another bioactivity test carried out was PG's anticancer activity. Cancer is a major threat to humanity and has become a global burden since 10 million cancer-related deaths were recorded in 2020 (Shanmugam *et al.,* 2024). Cancer can develop almost anywhere in the body. The causes of cancer include host factors such as genetics, epigenetics, microbiome, age, gender, metabolic conditions, inflammatory conditions, and immune function (Mohamed *et al*., 2021). Various classes of anticancer drugs have been developed, many of which are of natural origin. Natural products are the mainstay of cancer chemotherapy, but most cancer drugs cause unwanted side effects due to their lack of tumor specificity and multidrug resistance. The search for potent, safe, and selective anticancer compounds is essential for the development of new drugs, and natural products are particularly useful due to their excellent structural diversity for the construction of new compounds (Chauthe *et al.,* 2012). Kim *et al.* (2015) reported that PG has anticancer activity against breast cancer stem cells, which are more sensitive to anticancer drugs such as cisplatin, etoposide, taxol, and ionizing radiation, and decreases their ability to form spheroids. PG-derived dimer compounds have also been studied by Chauthe *et al*. (2012), who found that these compound has in vitro anticancer activity in various cell lines.

This review uses relevant literature published over the last two decades, from 2003 to 2025, to obtain up-to-date information on PG-derived compound research and its biological activity, and adds 1 additional literature source from 1995 that discusses the Houben–Hoesch method in full. Previous studies on PG-derived compounds (Singh and Bharate, 2006), derivatives of PG compounds of various genera (Bridi *et al*., 2018), PG-derived bioactivity, such as antibacterial (Peron *et al*., 2024; Shamsudin *et al.,* 2022), antibacterial and anticancer activity of PG cabonil (Bashir *et al*., 2023) have been documented by several reviews. However, discussions of various

PG derivatives, including comparisons of Fourier transform infrared (FTIR) and nuclear magnetic resonance (NMR) characterization, as well as their antibacterial, antioxidant, and anticancer bioactivities, have not been documented. This review brings together key insights from various reviews into a more comprehensive framework for the development of PG compounds, which could help researchers develop more effective new drugs.

PG COMPOUND AND THEIR DERIVATIVES

PG compounds are compounds in the natural phenolic class that are widely found in the genus Callopylum (Hertiningtyas *et al*., 2013). Singh and Bharate (2006) said that PG has been isolated from Eucalyptus kino, Acacia arabica, and marine algae, including the families Phaeophyceae, Fucaceae, Myrtaceae, and other families such as Guttiferae, Euphorbiaceae, Aspidiaceae, Compositae, Rutaceae, Rosaceae, Clusiaceae, Lauraceae, Crassulaceae, Cannabinaceae, and Fagaceae. PG derivatives are also found in brown plants and algae, such as gradinol, produced by some species of Eucalyptus, to the more complex florotanin found in the brown algal family. In addition, PG derivatives are produced by several microorganisms, and 429 PG derivatives have been isolated from the genus Hypericum (Biessy and Filion, 2021). The genus *Mallotus* (*Euphorbiaceae*), which is widely found in tropical Africa and Madagascar, is reported to be a rich source of biologically active compounds such as PG, flavonoids, steroids, benzopyrans, and cardenolides (Tchangoue *et al*., 2020). The compound resulting from polycyclic polyprenylated acylphloroglucinol (PPAP) is abundant in plants of the Guttiferae family, especially Hypericum ascyron Linn.

PG compounds, polyphenol compounds containing aromatic phenyl rings with 3 hydroxyl groups (Mondal *et al*., 2017). Unlike other phenolic compounds, PG serves as the basic framework for more than 600 secondary metabolites (Kumar *et al*., 2018). Structurally, PG has a very symmetrical shape, is part of the aromatic system, and contains many electrons, with 3 equal active sites. It is particularly advantageous for electrophilic aromatic substitution (Kusumaningsih *et al*., 2019). There are 2 forms of tautomer, namely 1,3,5-trihydroxybenzene (tautomer phenol) and 1,3,5-cyclohexanetrione (tautomer) (Yan *et al*., 2021), where two tautomers are zero and keto in equilibrium (Kusumaningsih *et al*., 2016). The PG form in the zero tautomer with 3 OH groups is more stable, due to the aromatic stability of the benzene ring. However, in the form of keto PG, it is easier to react because of the considerable carbon-oxygen double bond strength. According to Hartree-Fock theory, the tautomer zero 3 IH is predicted to be more stable than the keto form by up to 35 kcal/mol (Oziminski and Wójtowicz, 2020).

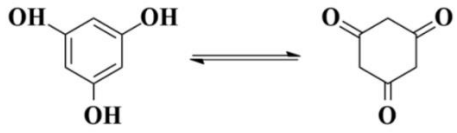

1,3,5-trihydroxybenzene 1,3,5-cyclohexanetrione

Figure 1. PG form and its tautomers (Kusumaningsih *et al*., 2016).

PG compounds are increasingly important because they exhibit various bioactivities, such as antioxidant, antimicrobial, anti-allergic, anti-inflammatory, insect-eating inhibition, anti-HIV (Kusumaningsih *et al*., 2016), anticancer (Chauthe *et al.,* 2012), and antifungal (Prasetyo *et al*., 2022). PG compounds and their derivatives are also used as secondary metabolites of plant materials (Mondal *et al*., 2017). PG has been shown to protect cells from H2O2-induced oxidative stress by activating catalase and to provide radioprotection against gamma radiation-induced cell damage by inhibiting oxidative stress (Kim *et al*., 2015). The bioactivity can be further enhanced by modifying the main compound into derivative compounds. Modifications can be made by adding new groups such as acyl, methyl, anhydric acid, alkyl nitrile, carboxylic acid, and others (Kusumaningsih *et al*., 2023; Singh *et al*., 2009).

Derivative products of PG compounds can be in the form of APG, PG dimer, PG trimer, tetrameric PG, phlorotanin, and others (Kusumaningsih *et al*., 2023; Singh *et al*., 2009). APG is the largest group of natural PGs. The most studied APG is gradinol, a PG derivative that contains isovaleril, formal, and methyl substituents. Silalized PG is also found in microorganisms. PG mono-, di-, tri-acetyl is reported to be present in *the bacterium Pseudomonas fluorescens* (Singh and Bharate, 2006). PG dimers are widely isolated from *Dryopteris* species, and their synthesis uses PG monomers as starting materials and aliphatic aldehydes as connecting molecules. Trimeric and tetrameric phloroglucinol can be synthesized using a similar approach to that for dimeric compounds. Phlorotanin has the highest molecular weight among PG group compounds. Its structural complexity is enormous

(Singh *et al*., 2009). Phlorotanin is composed of polymer chains of PG alkaline residues connected via C−C and/or C−O−C bonds. Phlorotanin is classified as fukol (phenyl bond), phloroetol (ether bond), fucophloroetol (ether and phenyl bond), eckol, fuhalol, and karmalol. The biological activities of phlorotanins include antioxidant, anticancer, antidiabetic, antiviral, antimicrobial, anti-inflammatory, and neuroprotective effects, with promising potential across various fields such as pharmaceuticals, food, and nutraceuticals (Yan *et al*., 2021).

Factors that affect the biological activity of a natural compound are hydroxyl (−OH) groups, hydrophobic substituents such as orenil groups, alkyl chains, heterocyclic groups containing nitrogen and oxygen (Xie *et al*., 2014), driving substituents (Lee *et al*., 2013), and molecular weight (Tan *et al*., 2017). Carbonyl groups (C=O) also play a role in the bioactivity of a compound (Suryani *et al*., 2020). The R group (side chain) can affect a compound's polarity and solubility, thereby influencing biological activity (Delfanian *et al*., 2021). In addition, modifications can involve the addition of other groups or metal compounds, which generally increase biological activity. In Table 1, FTIR and NMR spectra are compared from 51 PG-derived compounds.

Based on Table 1, compounds **(2 – 7)** are derivative compounds of PG results. The resulting compounds that bind to PG can be acetyl, isobutyryl, isovaleril, propionyl, and butyryl; they can be mono- or di-. Compared to compound **1**, the addition of the result is directly bound to the C2 and C6 aromatic rings. Acetyl substituent (compounds **2** and **5**) is characterized by the appearance of a shift in ^{1}H-NMR around δ_H 2 ppm, namely the methyl ketone group (McMurry, 2008). In isobutyryl, isovaleryl, and propionyl substituents **(3, 4, 6, and 7)**, the methyl group (CH3) appears at a δ_H shift of 0.9 – 1 ppm, which does not appear in compound **(1)**. Meanwhile, in FTIR absorption, there is a C=O group around 1600 cm^{-1} and C–H stretches at ~2900 cm^{-1}, indicating the presence of an outcome group in PG compounds (Nandiyanto *et al*., 2019). Compounds **(8 – 12)** are PG-derived compounds that have been modified by adding ninhydrin compounds through a synthesis process. The presence of additional compounds is indicated by NMR signals. The new signal in the form of aromatic C−H clearly suggests the presence of a new aromatic ring apart from PG, and in ^{13}C-NMR, there is the appearance of a C quarterner signal derived from the basic structure of the ninhydrin compound (Tara, 2023; Cahyani, 2023; Kundu *et al*., 2004). Although in FTIR it is not very obvious because the clusters in ninhydrin are similar to those of PG, a new peak at ~1100 cm^{-1} indicates the presence of a C−O ether bond between the PG hydroxy group and the carbonyl of the ninhydrin group (Nandiyanto *et al*., 2019). Compounds **(13)** in the form of PG dimers are characterized by a methylene (CH_2) absorption at 1476 cm^{-1} in the FTIR region and by an NMR signal at δ_H 3.74. This methylene absorption is mainly due to a bridge between the two PG monomers, indicating that a dimer has formed (Squirt *et al*., 2023). Compounds **(15 and 16)** are PG-derived compound that is α-pyrone linked via a methylene bridge that appears at a signal shift of δ_H ~ 3 ppm. PG in Compound **(15)** has an identical side group, 2,2-dimethyl-2H-piran, which fuses with the aromatic rings, producing signal shifts of 124.8 and 117.3 ppm. While compound **(16)** is identical to the presence of the 2,3-dihydro-2-(prop-1-en-2-il)furan group, characterized by the appearance of two δ_H singlets of 5.14 and 5.02 ppm associated with vinyl protons, two singlets at δ_H 3.00 and 3.32 ppm, and triplets at 5.40 corresponding to oxymetin protons (Caesaro *et al*., 2015). Compounds **(19**, **20**, **42**, **and 43)** are a derivative compound of PG results that undergo methylation. On compounds **(19** and **20)**, there is a shift in the δ_H signal of 3.55 ppm. Both compounds have a substituent in the form of a butyl group at δ_H 1.66 (2H, m); 3.05 (2H, s, J=7.5 Hz); 0.99 (3H, t (J=7.5 Hz), and ^{13}C-NMR C=O at 206.7 ppm, gem-dimethyl at 1.4 ppm (6H, s), and methyl 2.05 ppm (3H, s). Differences between compounds **19** and **20** are only on the R chain: **19** butyl and **20** Acetyl (Lee *et al*., 2009). Compounds **25** and **26** are derivatives of monocyclic aliphatic PG and of geranylated bicyclic PG.

Compounds (**32)** and (**33)** are complex derivatives of PG containing Ni(II) and phosphorus. In addition to ^{1}H-NMR and ^{13}C-NMR, ^{31}P-NMR is also used to detect the presence of forfor. Signal shifts appear at δ_P 187.34 and 147.7 for compounds (**32** and **33)** (García-Eleno *et al*., 2015). Compounds **(44** and **45)** are complex formalized PG result compounds. For compound (**44)**, there are additional substituents in the form of 4 formalin groups and terpenoid chains. There are formal groups that appear at the δ_H aldehyde proton signal shift of 9.9 (s), ~10.1 (s, 4H), and δ_C C=O 190.07 – 192.26. In addition to iu, PG connecting bridge carbon also appears with δ_H 2.88 (s) and 5.84 (s), respectively. while for compound (**45)**, PG derivatives are PG monomers attached to one sesquiterpene globulane with 2 formal groups. Formalyl groups appear at δ_H 10.06 (s, 2H) and δ_C 191.5 and 191.6. For sesquiterpene globulane, methyl groups appear at δ_H 0.68, 0.76, 0.78, 1.07, and 1.089 and δ_C 16.79 – 27.5. The terpene ring skeleton appears at δH signal shift 0.518 – 2.27, and there is a connecting bridge of proton signals at δ_H 3.4 and δ_C 35.4 (Soliman *et al*., 2014).

Table 1. NMR and FTIR analysis results of PG compounds and their derivatives.

Compounds	Structures	NMR	FTIR	Literatures
(1) Phloroglucinol	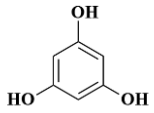 1	^{1}H-NMR δ ppm: H−C=C Ar (5.85)	−OH 3191 cm^{-1}, C=O 1618 cm^{-1}, C=C 1500 and 1407 cm^{-1}	(Jégou *et al*., 2015)
(2) MAPG (Monoacetyl phloroglucinol)	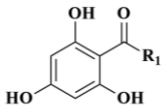 **2**: R = CH_3 **3**: R = $CH(CH_3)_2$ **4**: R = $CHCH_2(CH_3)_2$	^{1}H-NMR δ ppm: CH_3 (2.62 (s, 3H)), CH Ar (5.89 (d, J= 3.1 Hz 2H))	−OH 3527 – 3458 cm^{-1}, C−H stretching (ar) 3049 cm^{-1}, C−H stretching 2910 cm^{-1}, C=O 1625 cm^{-1}	(Cahyani, 2023) (Anggrahini, 2019)
(3) MBPG (Monoisobutyl phloroglucinol)	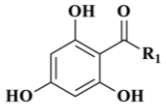 **2**: R = CH_3 **3**: R = $CH(CH_3)_2$ **4**: R = $CHCH_2(CH_3)_2$	-	−OH 3307 cm^{-1}, C−H stretching (ar) 2976 cm^{-1}, C−H stretching 2941 cm^{-1}, C=O 1727 – 1603 cm^{-1}	(Rahmaniar 2023)
(4) MVPG (Monoisovaleryl phloroglucinol)	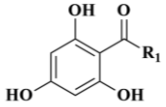 **2**: R = CH_3 **3**: R = $CH(CH_3)_2$ **4**: R = $CHCH_2(CH_3)_2$	^{1}H-NMR δ ppm: C−H Ar (5.88 (s, 2H)), CH_2 (2.94 (d, *J*=6.8 Hz, 2H)), CH (2.28 (m, 1H)), CH_3 (0.99 (d, *J*=6.6 Hz, 6H))	−OH 3367 – 3223 cm^{-1}, C−H 2957 and 2872 cm^{-1}, C−H 2927 cm^{-1}, C=O 1625 cm^{-1}	(Sholihah, 2023)

Table 1. NMR and FTIR analysis results of PG compounds and their derivatives (continued).

Compounds	Structures	NMR	FTIR	Literatures
(5) DAPG (Diaethyl phloroglucinol)	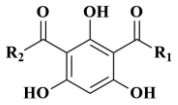 **5**: $R_{1,2} = CH_3$ **6**: $R_{1,2} = CH_2CH_3$ **7**: $R_{1,2} = CH_2CH_2CH_3$	^{1}H-NMR δ ppm: CH Ar (5.90 (s, 1H)), CH_3 (2.64 (s, 6H))	−OH 3366 cm^{-1}, C−H stretching (ar) 3060 cm^{-1}, C−H stretching 2920 – 2853 cm^{-1}, C=O 1602 cm^{-1}	(Cahyani, 2023; Anggrahini, 2019)
(6) DPPG (Dipropionyl phloroglucinol)	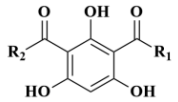 **5**: $R_{1,2} = CH_3$ **6**: $R_{1,2} = CH_2CH_3$ **7**: $R_{1,2} = CH_2CH_2CH_3$	^{1}H-NMR δ ppm: 13.09 (s, 2H), 5.91 (s, 1H), 3.06 (q, J=7.1 Hz, 4H), 1.07 (t, J = 7.2 Hz, 6H). ^{13}C-NMR δ ppm: C−OR (206.6), Ar−OH (170.6; 168.0), C−H (103.4), C−O (94.7; 36.7), CH_2 (8.4)	-	(Wang *et al*., 2025)
(7) PG Butyryl	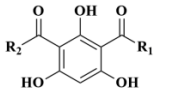 **5**: $R_{1,2} = CH_3$ **6**: $R_{1,2} = CH_2CH_3$ **7**: $R_{1,2} = CH_2CH_2CH_3$	^{1}H-NMR δ ppm: 5.80 (s, 1H), 3.07 (t, J=7.4 Hz, 4H), 1.72 (m, J=7.4 Hz, 4H), 0.99 (t, J = 7.4 Hz, 6H)	-	(Yang *et al*., 2024)
(8) PG-Hydrhydrin	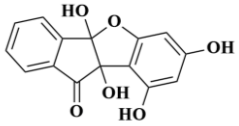 **8**	^{1}H-NMR δ ppm: Ar−H (7.97; 7.90; 7.80; 7.66), C=C (5.92; 5.82) ^{13}C-NMR δ ppm: C−OR (205.36; 204.55; 202.66), Ar−OH (172.39; 169.07; 164.57), CQ (111.46; 103.28; 97.23), C−O (81.77; 32.27), R−CH (135.94; 123.54; 105.02; 99.92)	−OH 3325 and 3465 cm^{-1}, C−H 3069 cm^{-1}, C=O 1735 cm^{-1}, C−O 1156 cm^{-1}, C−H Bending 742 cm^{-1}	(Shawn, 2023)

Table 1. NMR and FTIR analysis results of PG compounds and their derivatives (continued).

Compounds	Structures	NMR	FTIR	Literatures
(9) DAPG-Nihydrin	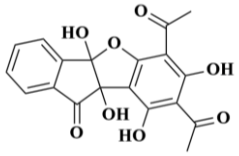 **9**	^{1}H-NMR δ ppm: Ar−H (7.83), −OH (77.34; 5.94), −CH_3 (2.62; 2.71) ^{13}C-NMR δ ppm: C−OR (205.36; 204.55; 202.66), Ar−OH (172.39; 169.07; 164.57), C−O (81.77; 32.27), R−CH (135.94; 123.54; 105.02; 99.92), Cq (32.27; 32.14; 30.77)	−OH 3233 cm^{-1}, C−H 2924 cm^{-1}, C=O 1720 and 1589 cm^{-1}, C−H bending 1220 cm^{-1}, C−O 1130 cm^{-1}	(Cahyani, 2023)
(10) MAPG-Ninhydrin	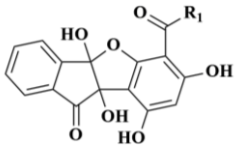 **10**: $R_1 = CH_3$ **11**: $R_1 = CH(CH_3)_2$ **12**: $R_1 = CHCH_2(CH_3)_2$	^{1}H-NMR δ ppm : Ar−H (8.03; 7.88), -OH (7.14; 2.09), −CH_3 (2.57)	−OH 3238 cm^{-1}, C−H 2925 cm^{-1}, C=O 1720 and 1618 cm^{-1}, C−H bending 1217 cm^{-1}, C−O 1142 cm^{-1}	(Cahyani, 2023)
(11) MBPG-Ninhydrin	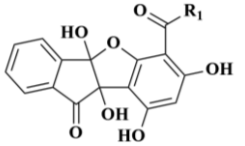 **10**: $R_1 = CH_3$ **11**: $R_1 = CH(CH_3)_2$ **12**: $R_1 = CHCH_2(CH_3)_2$	^{1}H-NMR δ ppm: Ar−H (8.98; 7.85; 7.76; 7.65), C=C (5.84), R−CH (1.3). ^{13}C-NMR δ ppm : C−O (81.87), C−H_3 (10.47, 13.47), C−H (22.76; 23.64), Cq (33.16; 38.78), C=C (111.87; 105,81; 123.56)	−OH 3352 cm^{-1}, C−H 2933 cm^{-1}, C=O 1717 and 1604 cm^{-1}, C−H bending 768 cm^{-1}, C−O 1148 cm^{-1}	(Rahmaniar, 2023)

Table 1. NMR and FTIR analysis results of PG compounds and their derivatives (continued).

Compounds	Structures	NMR	FTIR	Literatures
(12) MVPG-Ninhydrrin	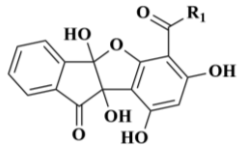 **10**: $R_1 = CH_3$ **11**: $R_1 = CH(CH_3)_2$ **12**: $R_1 = CHCH_2(CH_3)_2$	^{1}H-NMR δ ppm: Ar-H (7.99; 7.88; 7.73; 7.66), C=C (5.81), R−CH (0.94). ^{13}C-NMR δ ppm: C−O (51.71), C-H_3 (22.60; 22.38), C−H (29.84; 25.80), Cq (96.48), C=C (137.01; 131.90; 125.20; 123.65), C=O (205.90; 205.86)	−OH 3431 – 3215 cm^{-1}, C−H 2921 cm^{-1}, C=O 1725 cm^{-1}, C−H bending 776 cm^{-1}, C−O 1205 cm^{-1}	(Sholihah, 2023)
(13) DDAPG (Dimer Diaacetyl phloroglucinol)	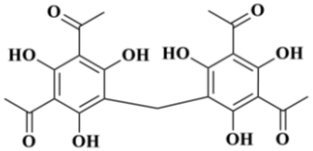 **13**	^{1}H-NMR δ ppm: CH_3 (2.73 (s, 6H) and 2.76 (s,6H)), CH_2 (3.74 (s, 2H)), OH (10.22 (s, −OH)) ^{13}C-NMR δ ppm: C=O (205,4 ppm), C−OH (170.7; 167.8; 165.3 ppm), CH_2 (15.22 ppm), CH_3 (33.4; 32.47 ppm).	OH 3205.8 cm^{-1}, C−H 2961.2 – 2858.6 cm^{-1}, CH_2 1476 cm^{-1}, C=O 1623.2 cm^{-1}, C=C Ar 1592.7 and 1423.5 cm^{-1}, C−O 1268.3 and 1181.5 cm^{-1}	(Kusumaningsih *et al*., 2023)
(14) Acronyculatin S	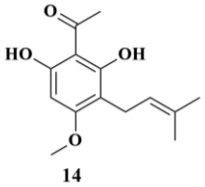 **14**	^{1}H-NMR δ ppm: Ar−H (6.01), CH_3 (2.66), CH_2 (3.33), C=C (5.18), CH_3 (1.77 and 1.83) ^{13}C-NMR δ ppm: C=C ar (162.7; 105.8; 159.1; 105.1; 165.6), C=O (203.3), C−H (21.2), C=C (121.3), CH_3 (25.6 and 17.7)	−OH 3371 cm^{-1}, C−H 2976 and 2927 cm^{-1}, C=O 1725 cm^{-1}, C−O 1278 and 1209, C−H bending 811 cm^{-1},	(Tchangoue *et al*., 2020)

Table 1. NMR and FTIR analysis results of PG compounds and their derivatives (continued).

Compounds	Structures	NMR	FTIR	Literatures
(15) (*S*)-3-[{5,7-dihydroxy-2,2-dimethyl-8-(2-methyl butanoyl)-2H-chromen-6-yl}methyl]-6-ethyl-4-hydroxy-5-methyl-2H-pyran-2-one.	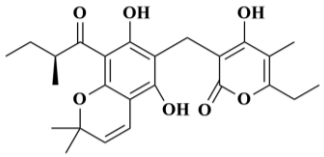 15	^{1}H-NMR δ ppm: OH (9.94 (s); 10.61 (s); 16.26 (s)), CH_2 (3.66 and 3.59), C−H Ar (5.43 (d); 6.68 (d)), CH3 (1.47 (s)). ^{13}C-NMR δ ppm: C=O (169.3; 210.9), C-O (169.3; 167.6; 159.0; 161.2; 161.9), CH_2 (17.4), CH Ar (124.8; 117.3), C-C Ar (102.0; 108.2; 104.0; 106.0; 104.4), CH_3 (27.8)	−OH 3216 cm^{-1}, C−H stretching Ar 2972 and 2935 cm^{-1}, C=O 1664 1 cm^{-1}, C=C Ar 1463, and 1424 cm^{-1}, C=OH 1360 cm^{-1}	(Casero *et al*., 2015)
(16) 3-[{4,6-Dihydroxy-7-(2-(*S*)-methylbutanoyl)-2-(prop-1-en-2-yl)-2,3-dihydrobenzofuran-5-yl}methyl]-6-ethyl-4-hydroxy-5-methyl-2H-pyran-2-one	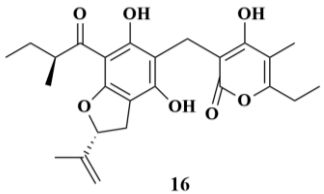 16	^{1}H-NMR: OH (8.52 (s); 14.0 (s); 10.37 (s)), CH_2 (3.59), C−H Ar (5.40 (t); 3.00 (dd), 3.32 (dd)), CH (5.14 (s); 5.02 (s)) ^{13}C-NMR: C=O (169.2; 211.9), C−O (169.2; 166.5; 161.5; 162.0; 160.0), C−C Ar (102.0; 108.1; 89.7; 99.9; 107.1; 103.4), CH_2 (18.2)	−OH 3343 cm^{-1}, C−H stretching Ar 2969 and 2878 cm^{-1}, C=O 1666 cm^{-1}, C=C Ar 1570 and 1432 cm^{-1}, C−OH 1379 cm^{-1}	(Casero *et al*., 2015)
(17) Biconjugation of 2,4 DAPG nanocomplex	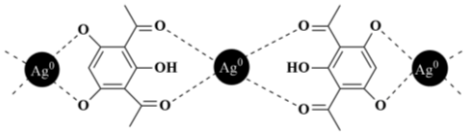 17	^{13}C-NMR δ ppm: C−C ar (94.58; 103.55; 168.60; 171.12), C=O (203.52), CH_3 (32.49)	−OH 3631.1 cm^{-1}, C−H stretching 2971.01 cm^{-1}, CH_3 2971 cm^{-1}, C=O 1738 cm^{-1}	(Syed *et al*., 2018)

Table 1. NMR and FTIR analysis results of PG compounds and their derivatives (continued).

Compounds	Structures	NMR	FTIR	Literatures
(18) Rhodomyrtosone B 6,8-dihydroxy-9-isobutyl-2,2,4,4-tetramethyl-5-(3-methylbutanoyl)-4,9-dihydro-1H-xanthene-1,3(2H)-dione	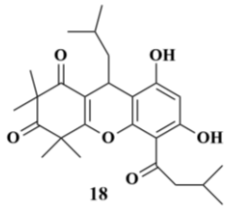 18	^{1}H-NMR δ ppm: OH (13.43), OH (6.4), CH Ar (6.23), isopentyl (4.25 (t); 1.38; 0.89; 0.87), isovaleril (3.18; 2.96; 2.37; 1.04) ^{13}C-NMR δ ppm: C=O (197.6 and 211.7), C=C Ar (159.0 and 159.9), CH_3 (24.3 (q); 24.4 (q); 24.8 (q); 25.4 (q))	OH 3372 cm^{-1}, C−H_3 2975, 2952 and 2868 cm^{-1}, C=O 1717, 1653 and 1622 cm^{-1}, C−C Ar 1468 cm^{-1}, C−O stretching 1385, 1256, and 1158 cm^{-1}	(Hiranrat and Mahabusarakam, 2008)
(19) Flavaspidic acid PB	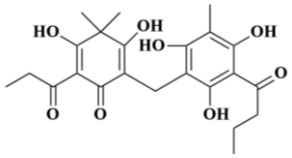 19	^{1}H-NMR δ ppm: CH_3 (0.99 (3H, t (*J*=7.5 Hz), 1.10 (3H, t (J=7.5 Hz), 2.05 (3H, s)), gem-dimethyl (1.40 (s, 6H)), CH2 (3.55 (s, 2H), 3.10 (s, 2H)), 1.66 (2H, m), 3.05 (2H, s, J=7.5 Hz). ^{13}C-NMR δ ppm: CH_3 (8.5; 8.1; 7.4), gem-dimethyl (24.7), C−OH (187.6; 171.7), C=O (156.4; 159.8, 198.3; 206.3), CH_2 (35.2; 45.8; 18.1; 16.2)	-	(Lee *et al*., 2009)
(20) Flavaspidic acid AB	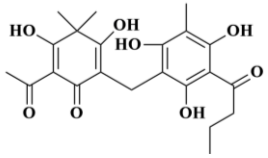 20	^{1}H-NMR δ ppm: CH_3 (0.91 (3H, t (*J*=7.3 Hz), 2.38 (3H, t), 1.87 (3H, s)), gem-dimethyl (1.16 (s, 6H)), CH_2 (1.60 (m, 2H), 3.04 (2H, t)), CH_3 Ar 1.87 (s, 3H), CH_2 (3.55 (s, 2H)). ^{13}C-NMR: CH_3 (13.8 and 8.1), gem-dimethyl (25.6), CH_3 Ar (7.9), C−OH (187.6; 171.7), C=O (156.4; 159.8, 198.3; 206.3), CH_2 (16.2)	-	(Lee *et al*., 2009)

Table 1. NMR and FTIR analysis results of PG compounds and their derivatives (continued).

Compounds	Structures	NMR	FTIR	Literatures
(21) *Eucalyprobusal I* 2,4,6-trihydroxy-5-((S)-1-((1S,6R)-6-isopropyl-3-methyl-2-oxocyclohex-3-en-1-yl-3-methylbutyl) isophthalaldehyde	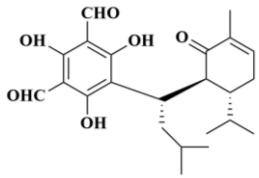 **21**	^{1}H-NMR δ ppm: CH_3 (0.08 (d) and 0.84 (d)), CH Ar (2.61 (d), 2.21 (d), and 6.94 (d)), -OH (12.68 (s), 13.60 (s), and 13.68 (s)) ^{13}C-NMR δ ppm: C−O Ar (168.6; 169.6; 167.9), CH (29.3), C=O Ar (206.8), CH_3 (21.5; 23.8; 16.2; 21.4)	OH 3431 cm^{-1}, C−H 2926, and 2856 cm^{-1}, C=O 1630 cm^{-1}, C−O 1306, 1182 and 846 cm^{-1}	(He *et al*., 2025)
(22) Mallophilol A	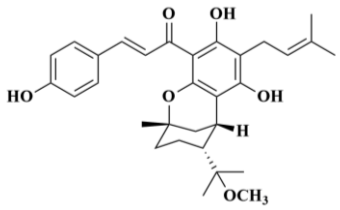 **22**	^{1}H-NMR δ ppm: H-C=C (7.86 (d) and 7.68 (d)), CH_3 (1.79 (s); 1.66 (s); 1.44; 0.78), OH (14.12 (s); 9.32 (s)), OCH_3 (3.40 (s)) ^{13}C-NMR δ ppm: C=O (193.1), C−O (157.2; 163.4; 159.6), Cq (105.6; 108.5; 102.1), C=C Ar (129.1; 130.1; 116.0), CH_3 (40.1; 22.2; 19.3; 26.0; 29.0)	OH 3530, 3445, and 3391 cm^{-1}, C=O 1670 cm^{-1}, C=C Ar 1563 cm^{-1}, C−O stretching 1380, 1355, 1315, 1155, and 1054 cm^{-1}	(Chen *et al*., 2024)
(23) Mallophilol D	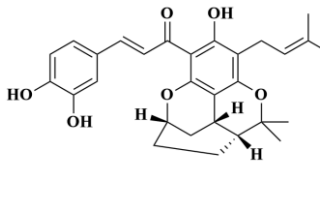 **23**	^{1}H-NMR δ ppm: H−C=C (7.86 (d) and 7.61 (d)), CH_3 (1.97 (d); 1.59 (s); 22.2; 1.50), OH (14.60 (s)). ^{13}C-NMR δ ppm: C=O (191.4), C−O (162.7; 160.7; 156.2; 145.8; 148.7), Cq (105.5; 109.5; 106.5), C=C Ar (123.3; 126.6), CH_3 (36.8; 21.6; 24.1; 28.5)	OH 3473 and 3428 cm^{-1}, C−H Ulur 2978, 2924, and 2772 cm^{-1}, C=O 1639 and 1519 cm^{-1}, C=C Ar 1448 cm^{-1}, C−O Ulur 1372 and 1276 cm^{-1}	(Chen *et al*., 2024)

Table 1. NMR and FTIR analysis results of PG compounds and their derivatives (continued).

Compounds	Structures	NMR	FTIR	Literatures
(24) Guajamer C	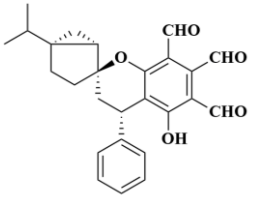 24	^{1}H-NMR δ ppm: OH (13.55 (s) and 13.20 (s)), CHO (10.10 (s) and 10.15 (s)), CH_3 (0.97 (d) and 0.91 (d)), CH Ar (7.15 (d), 7.28 (d), 7.19 (t), 7.28 (d)) ^{13}C-NMR δ ppm: C−O (168.6; 164.3; 169.8), CHO (192.2 and 191.6), Cq Ar (103.1; 104.; 104.0), CH_3 (19.7 and 20.1)	OH 3061 and 3026 cm^{-1}, C−H stretching 2957 and 2872 cm^{-1}, C=O 1629 cm^{-1}, C=C Ar 1442 cm^{-1}, C−OH 1384 and 1305 cm^{-1}	(Huang *et al*., 2021)
(25) 1-(5,7-Dihydroxy-2-methyl-2-(4-methylpent-3-en-1-yl)chroman-8-yl)ethone	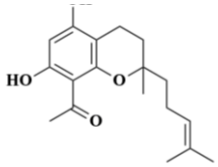 25	^{1}H-NMR δ ppm: 13.87 (s, 1H), 6.33 (s, 1H), 5.95 (s, 1H), 5.09 (ddd, J ¼ 7.1, 4.1, 1.2 Hz, 1H), 2.64 (s, 3H), 2.63 – 2.55 (m, 2H), 2.10 – 2.02 (m, 2H), 1.95 – 1.63 (m, 5H), 1.60 (s, 3H), 1.35 (s, 3H). ^{13}C-NMR δ ppm: COR (203.6), Ar−OH (164.8; 160.7), 157.6; 132.2; 123.7; R_3−CH (106.3; 99.9; 95.2), C−OH (78.4), Cq (39.6; 33.4; 29.4), CH_3 (25.7; 24.2; 22.6 and 17.6).	-	(Sun *et al*., 2014)

Table 1. NMR and FTIR analysis results of PG compounds and their derivatives (continued).

Compounds	Structures	NMR	FTIR	Literatures
(26) (E)-1-(3-(3,7-Dimethylocta-2,6-dien-1-yl)-2,4,6-Trihydroxy phenyl)ethenone	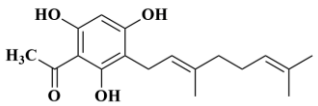 **26**	^{1}H-NMR δ ppm: 11.41 (s, 1H), 8.62 (s, br, 1H), 6.35 (s, 1H), 5.86 (s, 1H), 5.25 (dd, J ¼ 7.2, 6.0 Hz, 1H), 5.13 – 4.97 (m, 1H), 3.37 (d, J ¼ 7.1 Hz, 2H), 2.67 (s, 3H), 1.81 (d, J ¼ 0.9 Hz, 3H), 1.67 (s, 3H), 1.59 (s, 3H).	-	(Sun *et al*., 2014)
		^{13}C-NMR δ ppm: COR (203.8), Ar−OH (162.4; 161.4; 160.4), R3−CH (140.0; 132.2; 123.6; 121.4; 95.3), Cq (39.7; 32.9; 26.3; 25.7), CH_3 (21.5; 17.7; 16.2)		
(27) all-(Z)-5',7'-dihydroxy-2-(4,7,10,13,16 nonadecapentaenyl)chromone	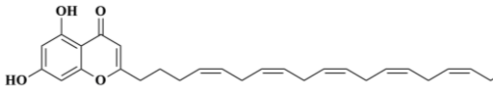 **27**	^{1}H-NMR δ ppm: CH Ar (6,06 (s, 1H); 5.35 (s, 1H); 6.29 (d, 1H)), CH_2 (1.78 (quint, 1H); 2.17 (q, 1H)), CH (5.31-5.46(m, 1H); 5.31 – 5.46 (m, 1H)), CH_3 (0.96 (t, 3H), OH (12.53 s)	-	(Hamiche *et al*., 2021)
		^{13}C-NMR δ ppm: C−O (170.55), C=C Ar (107.80), C=O Ar (182.58), C−OH (158.29 and 162.54), C=C (99.42, 94.15; 105.10; 162. 4; 129.31; 128.58; 128.43; 127.90; 128.30), C−C (33.64; 26.64; 26.42; 25.25; 25.61; 25.63), CH_3 (14.26).		

Table 1. NMR and FTIR analysis results of PG compounds and their derivatives (continued).

Compounds	Structures	NMR	FTIR	Literatures
(28) PHB 2,7"-phloroglucinol-6,6'-bieckol	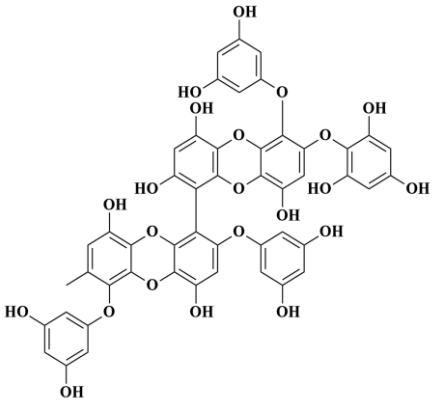 **28**	^{1}H-NMR δ ppm: CH Ar (5.57 – 6.25 ppm) ^{13}C-NMR δ ppm: C−C Ar, C=C Ar (95.2 – 160.2), and C−OH (137 – 160,3)	-	(Kang *et al*., 2012)
(29) PPB pyrogallol-phloroglucinol-6,6'-bieckol	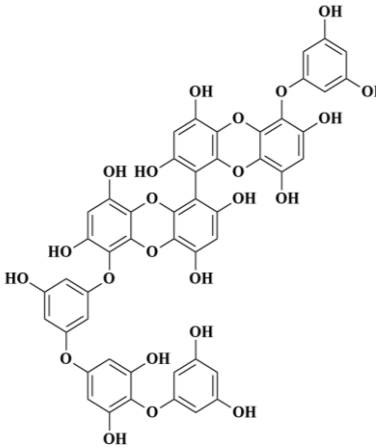 **29**	^{1}H-NMR δ ppm: CH Ar (5.54 – 6.25) and OH (8.25 – 9.87) ^{13}C-NMR δ ppm: C−C Ar, C=C Ar, and C−OH (94.4 – 162.9)	-	(Kang *et al*., 2011)

Table 1. NMR and FTIR analysis results of PG compounds and their derivatives (continued).

Compounds	Structures	NMR	FTIR	Literatures
(30) Kitosan-PG conjugate	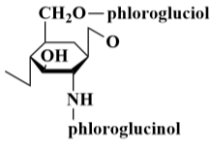 **30**	^{1}H-NMR δ ppm: CH_3 2.00, CH Ar (3.14 and 4.83), pyranose rings (3.14 and 4.30), CH Ar (PG) (6.30 and 7.58).	-	(Woo and Je, 2013)
(31) 2,4,6-triacetylphloroglucinol (TAPG)	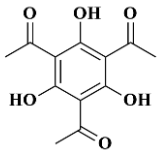 **31**	^{1}H-NMR δ ppm: 8.11 (s, 1H), 2.71 (s, 1H)	OH 3472.41 – 3356 cm^{-1}, Csp3-H 3000 − 2800 and 1367 cm^{-1}, C=O 1623 cm^{-1}, C−OH 1418 cm^{-1}, C−O 1299 cm^{-1}	(Kusumaningsih *et al*., 2019)
(32) POCOP-Ni(II) pinch compounds (Pr)	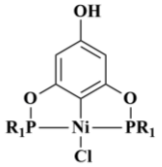 **32: R_1 = 'Pr**	^{1}H-NMR δ ppm:1.3 (m, 24H), 2.32 (m, 4H), 5.93 (s, 2H). ^{13}C-NMR δ ppm: CH_3 (16.9; 17.6; 27.9), C−OH (94.0 and 114.0), Ar−OH (157.9 and 169.0) ^{31}P-NMR δ ppm: 187.34.	OH 3285 cm^{-1}, C−H 2929 and 2870 cm^{-1}, C=C Ar 1598 cm^{-1}	(García-Eleno *et al*., 2015)
(33) POCOP-Ni(II) pinch compounds (Ph)	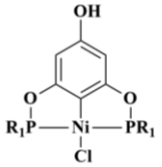 **33: R_1 = Ph**	^{1}H-NMR δ ppm: 6.9 (s, 2H), 7.2 (m, 20H). ^{13}C-NMR δ ppm: C−OH (95.3), R3−CH (128.3; 128.5; 128.9; 131.1; 131.6; 131.7; 132.5) ^{31}P-NMR δ ppm: 147.7	−OH 3293, 3051, and 3074 cm^{-1}	(García-Eleno *et al*., 2015)

Table 1. NMR and FTIR analysis results of PG compounds and their derivatives (continued).

Compounds	Structures	NMR	FTIR	Literatures
(34) Phloroglusinol Ag nanoparticle	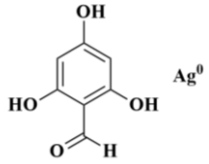 34	-	−OH 3400 and 2900 cm^{-1}, Nano Ag from PG 3400 – 2900 cm^{-1}, R−CHO 1500 – 1000 cm^{-1}	(Kumar *et al*., 2018)
(35) pyridine-3-yl-methylene-bis-(3-isopentanoyl-5-formyl-2,4,6-trihydroxybenzene)	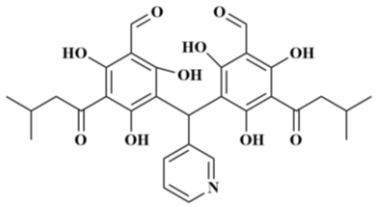 35	^{1}H-NMR δ ppm : 9.89 (s, 2H), 8.38 (d, J = 5.3 Hz, 2H), 7.78 (d, J= 5.3 Hz, 2H), 2.86 (d, J = 5.4Hz, 4H), 2.14 (m,2H), 0.87(d, J = 6.6 Hz, 12H). ^{13}C-NMR δ ppm: COR (206.9; 194.9; 191.8), Ar−OH (173.4; 164.4; 145.3), R3=CH (126.1; 108.3), Cq (53.9; 34.6; 31.1; 26.6; 23.5)	-	(Chauthe *et al*., 2012)
(36) 3,5-dimethoxyphenyl 4-methyl benzenesulfonate	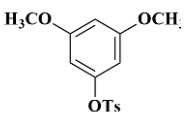 36	^{1}H-NMR δ ppm: 2.42 (*s*, 3H), 3.64 (*s*, 3H), 5.80 (*s*, 1H), 6.07 (*t*, 1H), 6.14 (*t*, 1H), 6.27 (*t*,1H), 7.30 (*d*, 2H), 7.73 (*d*, 2H). ^{13}C-NMR δ ppm: 21.7, 55.5, 100.6, 100.8, 102.5, 128.5, 129.8, 132.3, 145.6, 150.9, 157.2, 161.1.	-	(Chapman *et al*., 2008)

Table 1. NMR and FTIR analysis results of PG compounds and their derivatives (continued).

Compounds	Structures	NMR	FTIR	Literatures
(37) 2,4,6-trimethoxy-N-((4-methylpyrimidin-2-yl)carbamoyl)benzamide	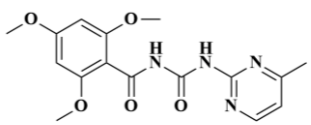 37	^{1}H-NMR δ ppm: 8.27 (d, J = 7.5 Hz, ^{1}H, pyrimidine-H), 7.02 – 7.00 (m, 1H, pyrimidine-H), 6.35 (s, 2H, Ar–H), 3.91 (s, 6H, OCH_3), 3.85 (s, 3H, OCH_3), 2.32 (s, 3H, CH).	-	(Zhang *et al*., 2022)
(38) 1-(3-(3-butyryl-2,6-dihydroxy-4-methoxy-5-methylbenzyl)-2,4-dihydroxy-6-methoxy-5-methylphenyl)-2-methylbutan-1-one	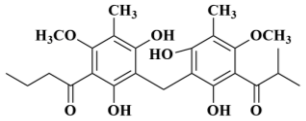 38	^{1}H-NMR δ ppm: OH 15.58 (s); 958 (d); 15.61 (s); CH_2 3.86 (s) ^{13}C-NMR δ ppm: C-OH (160.1, 161.1, 159.6 ppm), CH_2 (18.2), C=O 206.9	OH 3252 cm^{-1}, CH stretching 2927 cm^{-1}, C=O 1605 cm^{-1}, and C–C Ar 1459 cm^{-1}	(Tang *et al*., 2017)
(39) 1-(3-(2,6-dihydroxy-3-isobutyryl-4-methoxy-5-methylbenzyl)-2,4-dihydroxy-6-methoxy-5-methyl phenyl)butan-1-one	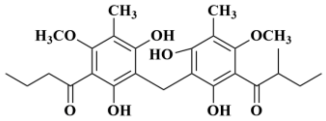 39	^{1}H-NMR δ ppm: OH 15.58 (s); 9.58 (d); 15.57 (s); CH_2 3.8 (s) ^{13}C-NMR δ ppm: C–OH (160.7, 161.7, 159.6 ppm), CH2 18.2; C=O 206.9.	OH 3255 cm^{-1}, C–H 2968 cm^{-1}, C=O 1605 cm^{-1}, and C–C Ar 1457 cm^{-1}	(Tang *et al*., 2017)
(40) 2,4-bis ((3R,5aS,6R,8aS,9R,10R,12R,12aR)-3,6,9-trimethyldecahydro-3H-3,12-epoxy[1,2]dioxepine[4,3-i]isochromen-10-yl)benzene-1,3,5-triol	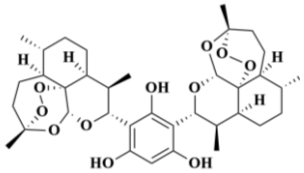 40	^{1}H-NMR δ ppm: 9.30 (s, 1H), 8.36 (d, 2H), 5.85 (s, 1H), 5.61 (d, *J* = 12.3 Hz, 2H), 5.04 (dd, *J* = 11.1, 5.2 Hz, 2H), 2.58 (dd, *J* = 11.2, 5.2 Hz, 2H), 2.26 (t, *J* = 12.3 Hz, 2H), 2.04 (d, *J* = 13.1 Hz, 2H), 1.91–1.78 (m, 2H), 1.67 (d, *J* = 12.4 Hz, 6H), 1.59 – 1.46 (m, 4H), 1.40 – 1.30 (m, 8H), 1.25 (dd, *J* ^{13}C-NMR δ ppm: 156.5, 155.1, 154.4, 104.6, 103.8, 96.0, 91.6, 91.4, 81.7, 81.6, 71.1, 51.6, 45.7, 45.6, 36.8, 36.7, 36.0, 34.2, 31.8, 31.2, 25.02-26.05, 20.8, 20.7, 20.5, 20.5, 13.7, 13.6.	OH 3379 cm^{-1}, C–H 2927 – 2872, C=O 1632 cm^{-1}, C=C 1454, 1377, 1197, 1135, 1112, 1038, 878 cm^{-1}	(Xu *et al*., 2023)

Table 1. NMR and FTIR analysis results of PG compounds and their derivatives (continued).

Compounds	Structures	NMR	FTIR	Literatures
(41) 5-hydroxy-4,6-bis ((3R,5aS,6R,7aS, 8R,9R,11R,11aR)-3,6,8-trimethyl decahydro-3,11-epoxypyrano[3',4':1,5]cyclopenta[1,2-c][1,2] dioxepin-9-yl)-1,3-phenylene diisopropyl dicarbonate	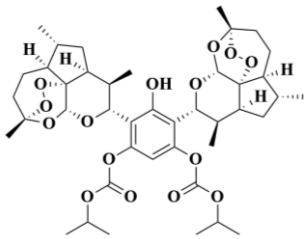 **41**	^{1}H-NMR δ ppm: *δ* 8.88 (s, 1H), 6.69 (s, 1H), 5.77 (s, 1H), 5.35 (s, 1H), 5.07 (d, *J* = 11.0 Hz, 1H), 4.91 (dd, *J* = 16.5, 8.8 Hz, 2H), 4.79 – 4.71 (m, 1H), 3.02 (d, *J* = 3.9 Hz, 1H), 2.64 (s, 1H), 2.24 (d, *J* = 35.3 Hz, 2H). ^{13}C-NMR δ ppm: *δ* 155.0, 152.1, 152.0, 150.7, 147.5, 118.6, 115.0, 109.6, 105.0, 103.5, 92.2, 91.6, 81.6, 80.8, 73.7, 72.6, 45.9, 45.3, 36.6, 36.4, 35.9, 34.3, 34.1, 30.5, 29.9, 26.2, 25.9, 24.9, 13.6, 13.3	OH 3362 cm^{-1}, C−H stretching 2928 – 2873 cm^{-1}, C=O 1763, C−C Ar 1629, 1605, 1378, 1240, 1038, 915.	(Xu *et al*., 2023)
(42) 2-butyryl-6-(3-butyryl-2,4,6-trihydroxy-5-methylbenzyl)-3,5-dihydroxy-4,4-dimethylcyclohexa-2,5-dienone	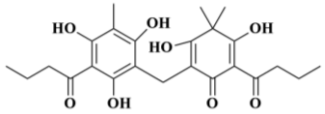 **42**	^{1}H-NMR δ ppm: 3.34 (s, 2H), 3.05 (t, J = 7.3 Hz, 2H), 2.78 (t, J = 7.6 Hz, 2H), 1.88 (s, 3H), 1.58 – 1.51 (m, 4H), 1.17 (s, 6H), 0.91 (t, 6H). ^{13}C-NMR δ ppm: 207.1, 199.2, 192.4, 188.1, 172.3, 160.4, 160.4, 111.8, 108.6, 106.1, 102.6, 46.3, 44.7, 39.8, 30.1, 19.9, 18.7, 18.6, 17.5, 16.7, 14.5, 14.4, 8.1.	OH 3135 cm^{-1}, C−H stretching 2961 cm^{-1}, C=O 1607 cm^{-1}, C−C Ar 1475, 1394, and 1196 cm^{-1}	(Yan *et al*., 2021)

Table 1. NMR and FTIR analysis results of PG compounds and their derivatives (continued).

Compounds	Structures	NMR	FTIR	Literatures
(43) 2-(3-Butyryl-2,4,6-trihydroxy-5-methylbenzyl)-3,5-dihydroxy-4,4-dimethyl-6-(3-methylbut anoyl)cyclohexa-2,5-dien-1-one	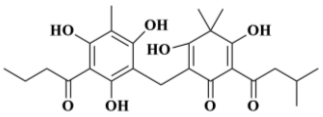 43	^{1}H-NMR δ ppm: 3.34 (s, 2H), 3.05 (t, J = 7.3 Hz, 2H), 2.72 (d, J = 7.0 Hz, 2H), 1.88 (s, 3H), 1.61 (d, J = 7.4 Hz, 1H), 1.22 – 1.15 (m, 2H), 1.16 (s, J = 3.2 Hz, 6H), 0.94 – 0.89 (m, 9H). ^{13}C-NMR δ ppm: 206.1, 199.2, 192.1, 187.5, 171.8, 160.1, 111.4, 108.4, 108.3, 102.2, 49.5, 45.8, 44.4, 26.8, 25.6, 22.9, 18.3, 16.3, 14.1, 7.6.	OH 3189 cm^{-1}, C−H stretching 2960 and 2873 cm^{-1}, C=O 1608 cm^{-1}, C−OH 1474 cm^{-1}, C−O 1196 and 1026 cm^{-1}, C−H 893 cm^{-1}	(Yan *et al*., 2021)
(44) Sideroxylonal B	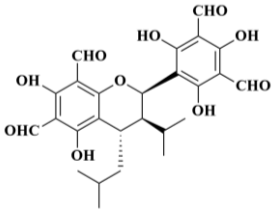 44	^{1}H-NMR δ ppm: 0.66 (3H, d), 0.87 (3H, d), 0.91 (3H, d), 1.01 (3H, d, J=56.0, H), 1.45 (1H, m), 1.52 (1H, m), 1.62 (1H, m), 1.90 (1H, m), 1.95 (1H, m), 2.88 (1H, dd), 5.84 (1H, d), 8.53 (1H, s), 9.96 (1H, s), 10.1 (1H, s), 10.14 (1H, s) and 10.17 (1H, s) ^{13}C-NMR δ ppm: 19.62, 20.96, 24.18, 25.54, 26.38, 26.62, 41.92, 44.63, 77.55, 100.45, 103.48, 103.97, 105.16, 108.21, 160.67, 167.43, 168.78, 169.43, 190.07, 191.95	-	(Soliman *et al*., 2014)
(45) Macrocarpal A	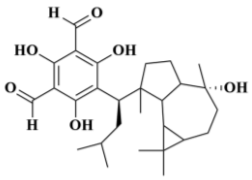 45	^{1}H-NMR δ ppm: 0.518 (1H, m), 0.54 (1H,m), 0.68 (3H, s), 0.76 (3H, d, J = 6.24,), 0.78 (3H, d, J=6.18), 0.92 (2H, m), 1.07 (3H, s), 1.089 (3H, s), 1.089 (3H, s), 1.12 (1H, m), 1.3 (1H, t),1.4 (2H, qd). ^{13}C-NMR δ ppm: 16.79, 18.8, 19.34, 20.1, 20.4, 21.4, 23.6, 24.15, 25.8, 35.12, 35.4, 43.7, 43.9, 48.19, 54.06, 105.1, 105.1, 109.17, 168.8, 169.22, 169.95.	-	(Soliman *et al*., 2014)

Table 1. NMR and FTIR analysis results of PG compounds and their derivatives (continued).

Compounds	Structures	NMR	FTIR	Literatures
(46) Eugenial D	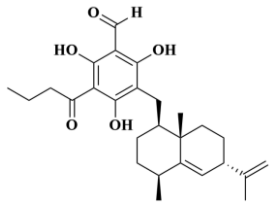 46	^{1}H-NMR δ ppm: OH (5.73, 14.35, 15.35), C=O (10.10 (s)), CH (2.65 (m) and 2.29 (dd)). ^{13}C-NMR δ ppm: C=O (206.9), C−O (161.5; 168.0; 171.9), C−C Ar (105.3; 104.1; 103.3)	OH 3505 cm^{-1}, C−H stretching 2960 and 2875 cm^{-1}, C=O 1625 cm^{-1}, C−C Ar 1437 and 1380 cm^{-1}	(Farias *et al*., 2018)
(47) Eugenial C	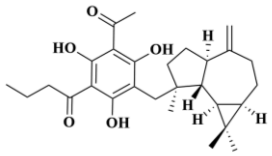 47	^{1}H-NMR δ ppm: OH (5.77; 14.42; 15.49), C=O (10.10 (s)), CH (2.28 (d) and 2.72 (d)). ^{13}C-NMR δ ppm: C=O (206,.9 and 192.1), C−O (162.1; 103.3; 104,1), C−C Ar (104.4; 103.3; 104.1).	OH 3503 cm^{-1}, C−H stretching 2960 and 2884 cm$^{-1,}$ C=O 1621 cm^{-1}, C−C Ar 1458 and 1380 cm^{-1}	(Farias *et al*., 2018)
(48) mono-O-acetyl dieckol	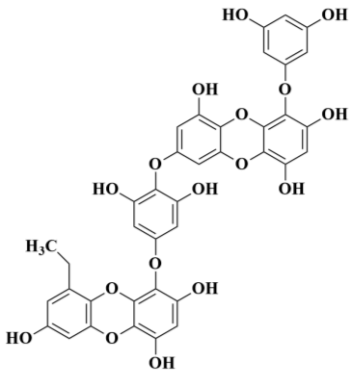 48	^{1}H-NMR δ ppm: OH (9.67 (s, 1H), 9.65 (s, 1H), 9.63 (s, 1H), 9.42 (s, 1H), 9.38 (s, 1H), 9.31 (s, 2H), 9.19 (s, 1H), 9.12 (s, 2H)), CH Ar 6.28 (d, J = 2.73 Hz), 6.22 (s, 1H), 6.16 (d, J = 2.73 Hz, 1H), 6.15 (s, 1H), 6.06 (d, J = 2.86 Hz, 1H), 5.92 (s, 2H), 5.81 (d, J = 2.86 Hz), 5.80 (t, J = 2.08 Hz, 1H), 5.73 (d, J = 2.08 Hz, 2H), 2.02 (s, 3H). ^{13}C-NMR δ ppm: C−OH (168.11 – 136.71), C=C (126.36 – 122.30), C-H (104.91, 101.01, 99.04), C−OH 98.81, 98.73, 96.63, 94.32)	-	(Shin *et al*., 2022)

This comparative review of characterization with FTIR and NMR uses analytical methods which are generally almost the same. There are variations in the completeness of the characterization; in addition, there are differences between the test compound, resulting from plant/algae isolation, and the compound synthesized by chemical reactions. About 50% of the studies present complete data from FTIR and NMR. In addition, the article only relies on one of the characterizations, with NMR or FTIR only. Presenting characterization data for only one method carries the risk of structural interpretation errors. In research by Kumar *et al*. (2018), it was claimed that the results of PG synthesis with Ag nanoparticles (AgNPs) were successfully confirmed based on FTIR data: –OH at 3400 and 2900 cm^{-1}, Nano Ag from PG at 3400 – 2900 cm^{-1}, and R–CHO at 1500 – 1000 cm^{-1}. However, without NMR data, it cannot be proven that the structure has been successfully formed. FTIR data reveal only the groups present in the compound, so the structural interpretation is less accurate. Research by Lee *et al*. (2009) only displays NMR data, claiming that the isolated compound was successfully obtained. The absence of FTIR data eliminates the presence of OH functional groups, which usually appear at ~3200 cm^{-1} and are difficult to detect by ^{1}H-NMR. This lack of data limits understanding of the bioactivity of functional groups and their possible interactions with those compounds. Therefore, this review highlights the submission of complete data that is at least useful for claiming the identification of new compounds or isolation results.

PG DERIVATIVE COMPOUND SYNTHESIS METHOD

PG compounds can be obtained by isolation and synthesis (Kusumaningsih *et al*., 2016). PG compounds and their derivatives are isolated from plants or microorganisms by extraction. Tchangoue *et al*. (2020) reported that *M. oppositifolius* leaves are rich in biologically active compounds, such as PG, which can be extracted by dissolving the leaves in a CH_2Cl_2/MeOH (1:1) mixture at room temperature for 48 hours. The resulting solution will be processed using various methods, such as purification by high-performance liquid chromatography (HPLC), thin-layer chromatography (TLC), and chromatography columns, to obtain the desired compound. PG-derived compounds, such as polyprenylated polyprenilate, resulting in Phloroglucinol (PPAP), can be obtained by refluxing dried twigs and leaves of *Hypericum ascyron* Linn with ethanol (Wang *et al*., 2024).

Some of the reported PG derivative synthesis methods include the Friedel-Crafts acylation method (Prasetyo *et al*., 2022). Friedel-Crafts itself consists of acylation and alkylation. The Friedel-Crafts acylation reaction is a change in the shape of a compound where there is an electrophilic substitution of aromatic compounds with an acylating agent, where there is more than one equivalent of acid catalyst (Sarvari and Sharghi, 2004). Friedel-Crafts acylation is one of the best methods for preparing aryl ketones, aromatic compounds to which the acyl group is added by treating them with an acidic agent in the presence of an acid catalyst. Commonly used asilating agents include halides, carboxylic acids, acid anhydrides, and others. This aylation reaction plays a major role in the synthesis of various aromatic ketones (Nayak *et al*., 2019). Friedel-Crafts acylation reactions offer advantages such as the absence of additional acids and bases, anhydrous conditions, and ease and economy for large-scale preparations (Sarvari and Sharghi, 2004). Friedel-Crafts acylation often requires more catalysts than the equivalent reaction (Reber *et al*., 2022).

Mono-, di-, and tri-formylated phloroglucinol can be obtained by phloroglucinol formylation, which has been reported using various formylation methods. The most conventional method is Vilsmeier-Haack formylation, which can produce mono- and di-formylated products under certain conditions, where the formylated species are chlorominium intermediates (Vilsmeier-Haack reagents) (Bashir *et al*., 2023). The Vilsmeier-Haack reaction is a method for introducing formal groups into various aromatic and heteroaromatic compounds, as well as heterocyclic compounds (Aneesa *et al*., 2012). This reaction uses efficient, affordable, and lightweight reagents such as dimethylformamide (DMF) and phosphorus oxychloride ($POCl_3$). Heterocyclic scaffolds are used as templates for the design, synthesis, and development of molecular or biologically active drugs. The structure of Vilsmeier-Haack reagents is important in medical chemistry due to their pharmacological activities, such as antibacterial, anticancer, anti-inflammatory, antifungal, antitumor, anti-HIV, and others (Chahal *et al*., 2023).

The Houben–Hoesch reaction is a common method for the aylation of electron-rich aromatic compounds (such as hydroquinone, phloroglucinol, or related ether derivatives) with nitriles, and it requires the presence of a strong Lewis acid or a Bronsted acid (Reber *et al*., 2022). These media almost always contain HCl or other protonic acids or water, which makes their properties complex and may make them very acidic. The Houben-Hoesch reaction of benzene typically yields a low yield of product. This reaction is difficult to analyze quantitatively due to the uncertainty of the reaction media's acidity. Using superacids will provide a medium with very high acid strength, stable, and better defined. This can overcome uncertainty about acidity and yield higher yields. Supersour

conditions will create a faster reaction rate, reduce by-products, and improve selectivity. However, using conventional acids such as H_2SO_4 results in low yields due to the formation of by-products. In addition, common acids have inconsistent reactions and are difficult to control (Sato *et al*., 1995).

Modification of PG compounds can be achieved by forming metal complex compounds. The metals that can be used are Ag^+, Ni(II), Cu(II), Co(II), Zn(II), Cd(II), and Fe(II) (Amaya-Flórez *et al*., 2024; Kusumaningsih *et al*., 2023; Nguyen *et al*., 2022; Van Nguyen *et al*., 2021). Many studies have used Ag, for example, Kumar *et al*. (2018) and Syed *et al*. (2018) have proven the ability of PG derivatives to act as effective reducing and stabilizing agents in the formation of AgNPs. Many methods have been proposed for the synthesis of environmentally friendly AgNPs, including plant-based, bacterial, ultrasonic, microwave, and room-temperature methods (Kusumaningsih *et al*., 2023). In the form of AgNPs, they offer many advantages due to their unique physicochemical properties, including their small size, large surface area-to-mass ratio, and ability to be functionalized with a variety of biological molecules (Aghapur *et al*., 2025). PG compounds are reacted with silver nitrate until a mixture is formed, then ultra-centrifuged to separate the bioconjugated nanocomplexes as a pellet (Syed *et al*., 2018). The −OH group in PG participates in situ in the reduction of Ag^+ ions, whereas the C=O group can form strong interactions with the AgNPs surface, thereby stabilizing the nanoparticles. As a type of natural phenolic compound, PG is an important key intermediate in the production of a broader range of compounds in various natural products and biologically active compounds (Kusumaningsih *et al*., 2023).

PG DERIVATIVES AS ANTIBACTERIAL COMPOUNDS

Antibacterial compounds are substances produced by organisms that inhibit bacterial growth or kill other microorganisms (Bota *et al*., 2015). Antibacterial compounds are effective based on the size of the inhibition zone they produce. This inhibition zone can depend on the ability of antibacterial compounds in substance diffusibility, the type of medium, and other factors. When a compound reacts with bacteria over a long period, it can exhibit both bacteriostatic and bacteriocidal properties (Rohdiana *et al*., 2013). Bacteria are categorized into Gram-positive and Gram-negative bacteria based on the arrangement of their cell walls. Some examples of gram-positive bacteria include *Staphylococcus, Streptococcus, Bacillus cereus,* and *Pseudomonas typhi.* Meanwhile, gram-negative bacteria such as *Escherichia coli, Pseudomonas,* and *Salmonella typhi* (Surahmaida and Lestari, 2019).

Antibacterial activity can be tested in vitro and in vivo. An in vivo method is a test conducted within an organism, while an in vitro method is a test conducted outside the organism, such as in a medium optimal for bacterial growth. Generally, antibacterial testing is carried out in *vitro* because the control conditions are better, interpretation is clearer, and less material is required (Jawetz *et al*., 2014). The *in vitro* method has several methods, such as disc diffusion test, well diffusion, point test, *cross-streaking* method, *food poisoning method*, agar *dilution*, macrodilution, and microdilution of broth, resazurin test, coculture method, time-kill kinetics, *flow cytometry,* thin-layer chromatography-bioautography (TLC), bioluminescence test, and impedance measurement (Hossain, 2024). The antibacterial activity of PG compounds and their derivatives is shown in Table 2.

Table 2. Antibacterial activity of PG comounds and their derivatives.

Compounds	Bacteria	Method	Results	Literatures
1	*S. aureus*	Obstruction zone	0 mm	(Shawn, 2023)
	MRSA		0 mm	
	E. coli		0 mm	
2	Concentration 100 µM	% inhibition	Inhibition:	(Nagel *et al*., 2012)
	B. subtilis (DSM 347)		100%	
	S. lentus (DSM 672)		97%	
	E. coli (DSM 498)		31%	
5	*MRSA*	MIC	3.91 µg/mL	(Yang *et al*., 2024)
	S. aureus		7.81 µg/mL	
	S. albus		15.63 µg/mL	
	B. subtilis		31.25 µg/mL	
6	MRSA	MIC	0.98 µg/mL	(Yang *et al*., 2024)
	S. aureus		3.91 µg/mL	
	S. albus		7.81 µg/mL	
	B. subtilis		1.95 µg/mL	

Table 2. Antibacterial activity of PG comounds and their derivatives (continued).

Compounds	Bacteria	Method	Results	Literatures
7	*MRSA* *S. aureus* *S. albus* *B. subtilis*	MIC	0.98 µg/mL 1.95 µg/mL 0.98 µg/mL 3.91 µg/mL	(Yang *et al*., 2024)
11	*S. aureus* *MRSA* *E. coli*	Buffer Zone	0 mm 0 mm 0 mm	(Rahmaniar, 2023)
12	*S. aureus* *MRSA* *E. coli*	Obstruction zone	0 mm 0 mm 7.2 mm	(Sholihah, 2023)
13	*Concentration 32 µg/mL* *S. aureus* *MRSA* *E. coli*	Obstruction zone	 8.71 mm 8.48 mm 0 mm	(Anggraini, 2019)
14	*P. aeruginosa* *S. aureus* *S. typhi* *E. coli*	MIC	3.12 µg/mL 6.25 µg/mL 6.25 µg/mL 6.25 µg/mL	(Tchangoue *et al*., 2020)
15	*E. coli* *S. aureus (VISA)* *S. aureus (MSSA)* *E. faecalis*	MIC	> 128 µM 64 µM 64 µM > 128 µM	(Casero *et al*., 2015)
16	*E. Coli* *S. aureus (VISA)* *S. aureus (MSSA)* *E. faecalis*	MIC	> 128 µM 64 µM 32 µM 64 µM	(Casero *et al*., 2015)
17	*B. subtilis (MTCC 121)* *E. coli* *P. aeruginosa (MTCC 7903)* *S. typhi (MTCC 733)* *S. aureus (MTCC 7443)*	MIC	0.97 µg/mL 0.97 µg/mL 1.25 µg/mL 0.97 µg/mL 1.25 µg/mL	(Syed *et al*., 2018)
18	*S. aureus* *E coli* *E. faecium* *P. acnes*	MIC	0.50 µg/mL >128 µg/mL 1.00 µg/mL 16.00 µg/mL	(Mo *et al*., 2021)
19	MICs 12-20 g/mL - *S. aureus KCTC 1916* - *B. subtilis KCTC 1914* *E. coli KCTC 1924* *Streptoccus mutans DSM 6178*	Obstruction zone	 16 mm 19 mm 11 mm 19 mm	(Lee *et al*., 2009)
20	MICs 12-20 g/mL - *S. aureus KCTC 1916* - *B. subtilis KCTC 1914* *E. coli KCTC 1924* *Streptococcus mutans DSM 6178*	Obstruction zone	 16 mm 15 mm 11 mm 18 mm	(Lee *et al*., 2009)

Table 2. Antibacterial activity of PG comounds and their derivatives (continued).

Compounds	Bacteria	Method	Results	Literatures
21	MIC 12.5 g/mL	Obstruction zone		(He *et al*., 2025)
	S. aureus ATCC 43300		12 mm	
	MRSA ATCC 43300		7 mm	
	S. aureus ATCC 29213		13 mm	
	S. epidermidis BCNN 102555		13 mm	
			8 mm	
	P. aeruginosa		7 mm	
	- A. baumanni ATCC 19606			
22	*MRSA*	MIC	> 48 µg/mL	(Chen *et al*., 2024)
	E. coli		> 48 µg/mL	
23	*MRSA*	MIC	12 µg/mL	(Chen *et al*., 2024)
	E. coli		48 µg/mL	
24	*S. aureus*	MIC	16 µmol/L	(Huang *et al*., 2021)
	S. epidermidis		8 µmol/L	
	E. coli		>32 µmol/L	

Flavonoids can be divided into several subclasses depending on their oxidative and substituent status. The antibacterial activity of flavonoids can be achieved in three ways: killing bacteria directly, synergistically enhancing the activity of antibiotics, and weakening bacterial pathogenicity (Xie *et al*., 2014). Many factors determine a compound's antibacterial activity. Clusters in a compound can increase biological activity, such as antibacterial activity. The compounds in Table 2 generally contain hydroxy, carbonyl, and R groups (side chains), which can determine their chemical properties and biological activity. The presence of an outcome group containing a carbonyl group (C=O) also plays a role as an antibacterial agent (Suryani *et al*., 2020).

On compounds **(19)**, phenolic hydroxyl groups commonly appear in the FTIR region ~3000 cm^{-1}, and carbonyl groups at ~1700 – 1600 cm^{-1} (Nandiyanto *et al*., 2019). These groups can form intramolecular hydrogen bonds, thereby improving electron delocalization and enhancing antibacterial activity. Thus, hydroxyl and carbonyl groups are important compounds in bioactivity. However, the addition of a methoxy group at any R position has been shown to reduce the antibacterial potential of these isolated compounds by inhibiting bacterial growth (Shamsudin *et al*., 2022). This hydroxyl group influences antibacterial activity by inhibiting bacterial growth. Compounds with weak hydroxyl groups exhibit high antibacterial activity because they enhance their ability to bind lipid membranes, enabling them to easily penetrate bacterial cell walls (Guidance *et al*., 2017). In addition, the existence of 2,2-dimethyl-2H-piran fused with aromatic rings that appear δ_C signal shifts of 124.8 and 117.3 ppm drastically reduces the activity contained in compounds **(15)** and **(16)** (Caesaro *et al*., 2015).

PG results showing increased lipophilicity in the tail can decrease antibacterial activity. There is an inverse relationship between the potential bactericidal activity and the lipophilicity of the tail as a result. When the tail results are longer than 14 carbons, it is almost insoluble in DMSO and shows weaker antibacterial activity. However, the tail results in a more lipophilic nucleus of acylfloroglusinol, and anti-MRSA activity increases dramatically, with the lipophilic ability of the resulting substituent comparable to the potential to inhibit bacterial growth. Therefore, the hydrophobicity or length of the resulting tail can be significantly optimized to modulate the antibacterial potential (Tan *et al*., 2017). It is evident that compounds **19** and **20** differ only in the side groups; the presence of butyl results in shifts in the δH signals for 3.10 (CH_2) and 1.10 (CH_3), whereas in 21 the acetyl groups give a δ_H signal at 2.38 (CH_3). The antibacterial activity of compound **20** is higher because butyl has better lipophilicity and size, allowing it to interact more effectively with bacterial membranes, especially in B. subtilis and Streptococcus mutans (Lee *et al*., 2009). A compound with a semipolar solvent will be more effective in inhibiting gram-positive bacteria such as *S. aureus* (Liswandari *et al*., 2018). Molecular weight can also affect antibacterial activity: the greater the molecular weight of a compound, the larger its molecular structure, making it more difficult to penetrate the bacterial cell wall (Tan and Lim, 2015). Compound **(7)** has very high antibacterial activity against Gram-positive bacteria, and the presence of a butyl group bearing a methyl group (CH_3) is observed at δ_H 0.9 – 1 ppm. The isobutyl group, represented by $–CH(CH_3)_2$, provides better compatibility with bacterial membranes than acetyl and isovaleryl groups (Prasetyo *et al*., 2023).

PG compounds complexed with metal compounds will exhibit increased bioactivity. As in the study by Syed *et al*. (2018), compound **(17)** exhibits very high antibacterial activity against both positive and negative bacteria.

Metal Ag, in the form of ions and AgNPs, is a broad-spectrum bactericide that does not cause resistance problems like some antibiotics (Flores *et al*., 2013). The positive charge of Ag^+ readily binds to the negatively charged bacterial cell walls via electrostatic attraction, leading to changes in permeability, respiratory disturbances, and leakage of intracellular contents. In addition, at higher concentrations, AgNPs can bind to the enzyme's thiol groups, inactivating most of the respiratory chain and leading to ROS formation, cell division, and cell death (Kusumaningsih *et al*., 2023).

Comparison of the antibacterial data in Table 2 is complicated by the use of gram-positive and gram-negative bacterial strains and by the methods used to measure antibacterial activity, such as inhibition zones and MIC values, which cannot be directly compared between compounds. However, in the literature, there is consistency regarding the presence of active antibacterial compounds bearing functional groups, such as OH and carbonyl, which appear in absorption bands at ~3200 cm^{-1} and ~1600 – 1700 cm^{-1} (Nandiyanto *et al*., 2019). The presence of aromatic rings also contributes to the antibacterial activity, as evidenced by δH signals at 5 – 7 ppm. These clusters are consistently present in compounds that are active as antibacterial, although methods vary.

PG DERIVATIVES AS ANTIOXIDANT COMPOUNDS

Antioxidant compounds are chemical compounds that have electrons that can be donated by one or more electrons (donor electrons) to free radicals, where the activity of free radical reactions is increased, resulting in the inactivation of oxidation reactions (Al Ridho *et al*., 2013). Antioxidant compounds can be classified into 2 groups based on their source: natural antioxidants and synthetic (artificial) antioxidants. Natural antioxidants of plant origin are phenolic compounds. While synthetic antioxidants are commonly used for food, namely Butyl Hydroxy Toluene (BHT), Butyl Hydroxy Anisol (BHA), tocopherols, and error profiles. The antioxidant activity of phenolic compounds is directly related to their chemical structure, including the position and number of hydroxyl groups and the degree of glycosylation. This compound contributes significantly to antioxidant activity by binding free radicals and chelating metals. The binding of free radicals reduces the formation of oxidation products and produces stable intermediates (Diniyah and Lee, 2020). The following PG compounds and their derivatives as antioxidant compounds are shown in Table 3.

Table 3. Table of antioxidant activity of PG compounds and their derivatives.

Compounds	Method	Results	Literature
(1)	DPPH	42 ± 1.00 µg/mL	(Archana and Vijayalakshmi, 2018)
	Superoxide anion	102 ± 2.00 µg/mL	
(2)	DPPH	14.88 µg/mL	(Triadmojo, 2021)
(3)	DPPH	23.10 µg/mL	(Prasetyo *et al*., 2023)
(4)	DPPH	38 µg/mL	(Sholihah, 2023)
(5)	DPPH	10 – 50 µg/mL	(Prasetyo *et al*., 2022)
(8)	DPPH	17.8 µg/mL	(Shawn, 2023)
(9)	DPPH	16.71 µg/mL	(Cahyani, 2023)
(10)	DPPH	17.92 µg/mL	(Cahyani, 2023)
(11)	DPPH	37.86 µg/mL	(Rahmaniar, 2023)
(12)	DPPH	23.9 µg/mL	(Sholihah, 2023)
(20)	DPPH	76.3 µM	(Lee *et al*., 2003)
	Superoxide Radical	64.4 µM	
	Lipid peroxidation	13.1 µM	
(25)	ORAC	22.5 ± 8.7 µM	(Sun *et al*., 2014)
(26)	ORAC	20.3 ± 5.2 µM	(Sun *et al*., 2014)
(27)	DPPH	89.91 ± 0.51 $µg/cm^{-3}$	(Hamiche *et al*., 2021)
(28)	DPPH	0.51 µM	(Kang *et al*., 2012)
	Alkyl radicals	2.07 µM	
	Superoxide Radical	57.19 µM	
(29)	DPPH	0.90 µM	(Kang *et al*., 2011)
	Alkyl radicals	2.54 µM	
	Hydroxyl Radical	62.93 µM	
	Superoxide Radical	109.05 µM	
(30)	DPPH	50.75 µg/mL	(Woo and Je, 2013)
(32)	TBARS	13.30 ± 0.77 µM	(Amaya-Flórez *et al*., 2024)
(33)	TBARS	19.29 ± 3.04 µM	(Amaya-Flórez *et al*., 2024)

Testing of antioxidant activity can be done by several methods based on different principles, such as 2,2-diphenyl-1-picrylhydrazyl (DPPH); peroxyl radical removal (Oxygen Radical Absorbance capacity, ORAC); Cupric Ion Reducing Antioxidant Capacity (CUPRAC); Total Radical-trapping Antioxidant Power (TRAP); removal of hydroxyl radicals; quantification of products formed during lipid peroxidation (Thiobarbituric Acid Reactive Substances, TBARS); Oxidation of Low-density Lipoproteins (LDLs), and others (Marinova and Batchvarov, 2011). Antioxidant activity is generally reported as an IC_{50} value. The IC_{50} value is the effective concentration of the extract needed to reduce 50% of the total DPPH, so that the value of 50 is substituted for the value of y. After substituting the value of 50 for the value of y, the value of x will be obtained as the value of IC_{50} (Tristantini *et al*., 2016). Some methods related to the value of the IC_{50} antioxidant category are shown in Table 4.

Table 4. IC_{50} values for antioxidant categories using several methods (Phongpaichit *et al*., 2007).

2,2-diphenyl-1-picrylhydrazyl (DPPH)		**Superoxide Anion Scavenging (Phongpaichit *et al*., 2007)**		**Hydroxyl radical scavenging**	
IC_{50} (µg/mL)	**Categories**	**IC_{50} (µg/mL)**	**Categories**	**IC_{50} (µg/mL)**	**Categories**
<10	Very powerful	<800	Very powerful	<2500	Very powerful
				2500 – 3000	Strong
10 – 50	Strong	800 – 1000	Strong	3000 – 4000	Medium
50 – 100	Medium	>1000 – 2000	Medium	4000 – 5000	Weak
100 – 250	Weak	>2000 – 3000	Weak	>5,000	Inactive
>250	Inactive	>3,000	Inactive		

PG compounds are the main phenolic compounds in *pistachio green hull* (PGH) water extract. The antiradical activity of PG increases with increasing antioxidant concentration from 10 M to 50 M. The antiradical activity of antioxidant compounds also depends on the number of electrons of hydroxy donors and carboxyl substitutions that increase the stability of phenoxyl radicals, where PG has three hydroxyl groups. An important role in the activity is also played by the intramolecular hydrogen bond (IHB) between the polar solvent and this functional group, which can contribute to the destruction activity of DPPH. The solubility and polarity of phenolic antioxidants increase molecular availability and mobility, thereby enhancing their ability to destroy free DPPH· significantly (Delfanian *et al*., 2021). The level of antioxidant activity is determined by its high lipid solubility, low toxicity, and more stable DPPH-derived radicals (Aini *et al*., 2010). An increase in the number of carbon atoms in the side group increases lipophilicity. Lipophilic compounds easily react with lipid radicals in emulsions and have higher antioxidant activity than hydrophilic compounds (Hamiche *et al*., 2021). However, the large structure of the compound can decrease antioxidant activity by creating a steric barrier that impedes the formation of free radicals in phenolic derivatives (Weng and Huang, 2014).

PG compounds containing aromatic result groups generally show higher antioxidant effects than monocyclic and bicyclic compounds with aliphatic result substitution (Sun *et al*., 2014). Factors that affect antioxidant activity include OH groups, carbonyl groups, heterocyclic groups, and propyl substituents (Lee *et al*., 2003). The more hydroxyl (OH) groups are bound to the aromatic ring in the compound, the more hydrogen atoms are given to neutralize free radicals so that their antioxidant properties increase (Prabawati, 2016). When the number of phenolic hydroxyl groups in a monomer is less than 4, the antioxidant activity is directly proportional to the number of phenolic hydroxyls. This means there is an optimal point; if more than 4, the antioxidant activity stops increasing or even decreases, depending on the spatial position of the molecule (Chen *et al*., 2020). In Table 2, compounds **(28)** and **(29)**, phlorotannin derivatives of bieckol, have very high antioxidant properties due to the numerous phenolic OH groups, which usually appear in the δC signal at ~160 ppm. Their activity is high despite their bulky structures because they possess multiple hydrogen donor sites that facilitate electron delocalization. In addition, the extensive conjugated aromatic system can neutralize radicals through resonance (Kang *et al*., 2012). The enthalpy of dissociation of the OH bond is very important for radical neutralization activity and is influenced by the nature of the electron donor in the ortho position. When the ortho position of the hydroxyl phenol, substituted by methoxy, hydroxyl, and amino groups, respectively, significantly contributes its electrons, thereby reducing the dissociation enthalpy of the Ar–OH bond and improving the radical stability of the phenolic hydroxyl group and antioxidant activity (Yang *et al*., 2021).

The substitutes for acyls and ninhydrin in the APG-Ninhydrin compound make the two compounds even more reactive in compounds (**8** – **12**). An acyl group is an electron attractant group capable of increasing the density of electrons in an aromatic ring. The R group in the result group is $–CH_3$, which usually appears in FTIR

as an aliphatic CH band at ~2900 cm^{-1}, belonging to a substituent group of electron donors that are aromatic-ring activators and can increase the rate of radical formation. The result group has a carbonyl group (C=O) that usually appears at ~1700 – 1600 cm^{-1}, and this functional group affects antioxidant activity. Carbonyl groups, as electron acceptors, can enhance electron delocalization, making the radicals formed upon neutralization of DPPH· more stable and conferring strong antioxidant properties (Noviany *et al*., 2023). Hamiche *et al*. (2021) reported that when carbonyl groups appear, a shift of the δ_C signal from 170.55 to 107.80 on the benzene ring conjugated to a double bond between C2 and C3 in compound (**27)** can increase antioxidant activity.

Table 3 indicates that antioxidant testing varies, so it cannot be directly compared between articles. The existence of a variety of antioxidant activity test methods can provide a more comprehensive picture, although the quantitative data obtained will differ. However, the groups that contribute to antioxidant activity are consistently present in the compounds listed in Table 3. The cluster, namely phenolic OH, appears in the FTIR region at ~3200 cm^{-1} (Nandiyanto *et al*., 2019) and in the ^{13}C-NMR signal at δ_C ~160 ppm (McMurry, 2008). This can strengthen the link between the compound's structure and its biological activity. The antioxidant strength category is already displayed in Table 4. Antioxidant activity is influenced by the ability of the constituent to delocalize electrons within the aromatic ring. The order of the constituent abilities is as follows: $-OH > -OCH_3 > -Br > -CO_2H > -CH_2\ CH_3 > -CH_3 > -CHO$ (Weng and Huang, 2014).

PG DERIVATIVES AS ANTICANCER COMPOUNDS

Cancer is a group of diseases characterized by the uncontrolled growth and spread of abnormal cells and is among the deadliest diseases worldwide (Ruiz-Torres, 2017). When cancer cells spread after incubation, cell proliferation has occurred. Bioactive compounds that significantly reduce proliferation have antiproliferative or anticancer activity. Anticancer activity focuses only on cancer stem cells (Yarley *et al*., 2021). Cancer cell death can be divided into two characteristic forms, namely apoptosis and necrotic cell death. Apoptosis is referred to as programmed cell death and is characterized by the maintenance of intact cell membranes during the process of cell suicide. Therefore, inducing apoptosis is a promising strategy for cancer prevention (Kong *et al*., 2009). The most common cancers are colorectal, breast, prostate, lung cancers (Ruiz-Torres, 2017), stomach, liver, and cervix (Rayan *et al*., 2017).

Various compounds, such as alkaloids, flavonoids, terpenoids, phenols, polysaccharides, saponins, and others, have been documented as natural bioactive products with potential anticancer activity. The majority (>60%) of clinically used anticancer drugs that have shown significant efficacy in treating cancer are derived from natural sources, including plants, marine organisms, and microorganisms. The anticancer activity of most natural ingredients often works through regulating immune function, inducing apoptosis or autophagy, or inhibiting cell proliferation (Rayan *et al*., 2017). The anticancer activity of phenolic compounds, namely PG-derived compounds, is shown in Table 5.

Cytotoxicity and anticancer testing methods can be performed using in vitro tests, including chromometric and fluorometric methods. The main difference between these two tests is the reagent used to estimate the total number of living cells based on dehydrogenase (mitochondrial) activity. Colorometric testing can be performed by several methods such as MTT (3-(4,5-Dimethylthiazol-2-yl)-2,5-diphenyltetrazolium bromide)/MTS **(**3-(4,5 dimethylthiazol-2-yl)-5-(3-carboxymethoxyphenyl)-2-(4-sulfophenyl)2H-tetrazolium), XTT test ((2,3-Bis-(2-methoxy-4-nitro-5-sulfophenyl)–2H-tetrazolium-5-Carboxanilide), violet crystal staining test (CVS), SRB (sulforhodamine B) test, and lactate hydrogenation test. Meanwhile, fluorescence-based testing can be performed using the Alamar Blue (AB) test, flow cytometry, the 5-Bromo-2′-deoxyuridine (BrdU) fusion test, the Annexin V test, and the Adenosine triphosphate (ATP) test (Sanjai *et al*., 2024).

Table 5. Anticancer activity of PG-derived compounds.

Compounds	Cancer Cells	Results	Literature
(31)	A549	57.51 ± 1.19 µM	(Mondal *et al*., 2017)
	MDA MB-231	81.48 ± 2.52 µM	
	HCT-15	124.50 ± 2.83 µM	
	HeLa	136.13 ± 1.49 µM	
(32)	U251	6.85 ± 0.08 µM	(Amaya-Flórez *et al*., 2024)
	K562	5.81 ± 0.20 µM	
	HCT-15	6.84 ± 0.90 µM	
	MCF-7	7.85 ± 0.60 µM	

Table 5. Anticancer activity of PG-derived compounds (continued).

Compounds	Cancer Cells	Results	Literature
	SK-LU-1	2.59 ± 0.20 µM	
(34)	MCF-7	78.03 ± 0.23 µ/mL	(Kumar *et al*., 2018)
(35)	ACHN	5.70 µM	(Chauthe *et al*., 2012)
	Panc1	6.10 µM	
	H460	5.80 µM	
	Calu1	6.30 µM	
	HCT116	5.50 µM	
	MCF1 0A	>30 µM	
(36)	C32 cells	48.7 ± 26.0 µM	(Chapman *et al*., 2008)
(37)	A-549	19.67 ± 0.27 µM	(Zhang *et al*., 2022)
	MCF-7	18.49 ± 0.18 µM	
	HeLa	29.73 ± 0.31 µM	
	HepG2	27.62 ± 0.31 µM	
(38)	A549	12.63 ±1.40 µM	(Tang *et al*., 2017)
	HCT-116	2.12 ± 0.16 µM	
	MDA-MB 231	7.50 ± 0.86 µM	
	PC-3	9.85 ± 1.08 µM	
(39)	A549	12.43 ± 0.93 µM	(Tang *et al*., 2017)
	HCT-116	5.44 ± 0.35 µM	
	MDA-MB 231	9.47 ± 0.70 µM	
	PC-3	14.29 ± 9.73 µM	
(40)	HeLa	0.029 µM	(Xu *et al*., 2023)
	K562	0.0034 µM	
	HepG2	0.049 µM	
	A549	0.121 µM	
	Raji	0.010 µM	
	Storm	0.028 µM	
(41)	HeLa	0.074 µM	(Xu *et al*., 2023)
	K562	0.052 µM	
	HepG2	1.117 µM	
	A549	2.519 µM	
	Raji	0.058 µM	
	Storm	0.164 µM	
(42)	A549	55.34 ± 0.87 µmol/L	(Yan *et al*., 2021)
	MCF-7	31.54 ± 1.03 µmol/L	
	HepG2	59.35 ± 0.93 µmol/L	
(43)	A549	42.31 ± 1.32 µmol/L	(Yan *et al*., 2021)
	MCF-7	73.59 ± 3.25 µmol/L	
	HepG2	105.75 ± 1.06 µmol/L	
(44)	HEP2	7.2 ± 0.50 µg/mL	(Soliman *et al*., 2014)
	MCF7	4.4 ± 0.25 µg/mL	
	CaCo	4.0 ± 0.36 µg/mL	
	10 FS	43 ± 0.80 µg/mL	
(45)	HEP2	14.8 ± 0.55 µg/mL	(Soliman *et al*., 2014)
	MCF7	7.8 ± 0.3 µg/mL	
	CaCo	11.4 ± 0.45 µg/mL	
	10 FS	50.1 ± 1.12 µg/mL	
(46)	K562	1.90 ± 0.10 µM	(Farias *et al*., 2018)
	Nalm-6	7.75 ± 0.40 µM	
	B16F10	3.20 ± 0.10 µM	
(47)	K562	0.38 ± 0.30 µM	(Farias *et al*., 2018)
	Nalm-6	10.5 ± 0.10 µM	
	B16F10	6.00 ± 0.30 µM	
(48)	A549	7.02 ± 1.53 µM	(Shin *et al*., 2022)
	NIH/3T3	481.41 ± 18.61 µM	

PG compounds are compounds shown to be effective against cancer stem cells (Shanmugam *et al*., 2024). This anticancer activity is also influenced by several factors, such as the functional group attached to the compound, its polarity, and lipophilicity. The anticancer properties of PG itself show an IC50 value of 235.31 ± 0.32 µg/mL, which is relatively low compared to those of its derivative compounds (Kumar *et al*., 2018). Xu *et al*. (2023) reported that antiproliferative activity, inhibiting cell growth, was inversely proportional to the length of the carbon chain substituent on the phenolic group—increased chain length and lipophilicity led to decreased activity. Toxicity to Vero cells decreases with increasing chain length. Compound **(36)**, with a pyridine-3-yl group on the connecting methylene and two diisovalerill PG groups, was found to be highly active in five cancer cell lines. Pyridine exhibits cytotoxicity against tumor and cancer cells due to the ortho position of the nitrogen atom, which results in methyl substitution on the pyridine ring (Mohamed *et al*., 2021). Compounds that have small alkyl substituents in the carbon methylene bonding are less active than compounds with large aromatic substituents. This shows that the substituents in the core compound that have a significant influence on anticancer activity are the dimeric PG core with long-chain acyl and formyl substituents and the connecting methylene carbon substituted with a large aromatic group (Chaute *et al*., 2012). The difference in the anticancer activity of the compounds, especially in compounds **(32)** and **(34),** is due to the steric factors of the alkyl groups located in the phosphorus atom appearing at δP 187.34 and 147.7, which can facilitate the release of chloride ions from the coordination plane, creating an empty space around the metal atom, allowing it to interact with specific biological targets. In addition, solubility can facilitate the optimal transport of these compounds (Amaya-Flórez *et al*., 2024).

PG derivatives containing tosylate groups have been shown to affect anticancer activity. While in **37** it has a tocylate group, which is active against C32 cells. This may indicate that the tocylate group plays an important role in the concentration or compartmentalization of compounds within the parasite. The presence of the tosyl group and its relative position are clearly important in all the cell types tested. The biological activity of a compound is related to its structure, not just its composition (Chapman *et al*., 2008). In addition, the electronic effects on the phenyl ring affect the anticancer activity. Compound **(36)** has a dimethoxyphenyl group, which promotes better anticancer activity (Mahapatra *et al*., 2021). Compound **(47)** contains tricyclic aromadendrene fragments, which are revealed to be 5 times and 13 times more potent than the bicyclic eudesmadiena fragment **(46)**. Eudesmadiena has larger terpenoidal (highly lipophilic) fragments bound to PG groups, which can cause the most potent cytotoxicity in both Nalm-6 and B16F10 cells (Farias *et al*., 2018).

In the Chauthe *et al*. (2012) study, PG dimers containing formalin substituents in aromatic groups exhibit good growth-inhibition properties, as evidenced by compound **(44)** having higher anticancer properties in HEP2, MCF7, CaCo, and 10 FS cells compared to compound **(45)**. It can kill cancer cells but only slightly damages normal cells, making it selectively active. The presence of formalin groups can also increase anticancer activity; compound 47 has 4 formal clusters, as evidenced by the δH values at 9.96, 10.1, 10.14, and 10.17. Four formyl groups serve as reactivity centers that chelate metal ions effectively and act as multi-targets between the 4 formyl groups and the aromatic system, enabling them to kill cancer cells effectively. Whereas compound 48 has only 2 formal compounds that appear on the signal δ_H 10.06 (s, 2H), in addition to δ_H signals 0.68, 0.76, 0.78, 1.07, and 1.089 and δ_C 16.79 – 27.5, indicating the presence of a sesquiterpene globulane group that causes very high lipophility and its molecular structure to become large, so that compound **(45)** has lower anticancer activity than compound **(44)** (Soliman *et al*., 2014).

The combination of PG compounds with metal nanoparticles can enhance their bioactivity. PG shows lower toxicity than compound **(34)**. The very high toxicity of compound **(34)** is mainly due to its smaller size (10 – 50 nm) and surface area (negative zeta potential), which affects intracellular damage (Kumar *et al*., 2018). This means that nanoparticles' activity depends on various parameters, such as size, shape, surface charge, and surface-bound molecules. The size of the nanoparticles is an important factor in determining final toxicity because the surface-to-volume ratio is high, increasing the number of atoms on the surface and the likelihood of contact. In addition, nanosized particles can readily cross the cell membrane and interact with intracellular components during the multiplication phase, ultimately leading to cell death (Kusumaningsih *et al*., 2023).

Based on the comparison data displayed in Table 5, there is a striking difference in the use of cancer cells and the testing method. The existence of this difference can provide a fairly broad knowledge of the results of qualitative tests. Compounds that have anticancer activity consistently have an active group in the form of aromatics appearing in ^{13}C-NMR δ_C signal 110 – 175 ppm and FTIR absorption at ~1500 cm^{-1} and phenolic OH groups that appear at FTIR uptake at ~3200 cm^{-1} (Nandiyanto *et al*., 2019; McMurry, 2008).

CONCLUSION

This review summarizes (1) Comparison of FTIR and NMR characterization of various PG-derived compounds, (2) Comparison of PG and its derivatives as antibacterial, antioxidant, and anticancer compounds. PG compounds and their derivatives are widely produced by plants, such as the nyamplung family Callophyllum, brown and marine algae, the family *Phaeophyceae*, *Fucaceae*, *Myrtaceae*, and others, and can be produced by derivatization synthesis methods. PG-derived compounds are widely researched and continue to develop because they play a very important role in the pharmaceutical industry and have the potential to become new drugs. Modification of PG compounds significantly affects their biological activity, properties, and characteristics, as well as their polarity. Characterization of compounds with FTIR and NMR to identify the structure of compounds. The bioactivity of PG derivative products can be in the form of antibacterial, antioxidant, anticancer, antiviral, anti-HIV, anti-fungal, and other activities. The presence of active side groups can increase or decrease its bioactivity. Side groups can be methoxy, diacetyl, hydroxyl, carbonyl, pyridine, and others. The longer the side group is, the more it can decrease bioactivity: the compound will be larger, its molecular weight will increase, it will be more lipophilic, and a steric barrier will inhibit the killing of disease cells.

CONFLICT OF INTEREST

There are no conflicts of interest in this article.

AUTHOR'S CONTRIBUTION

SV: Conceptualization, Original Script Writing, and Editing; TK: Supervision, Review, and Editing; MF: Supervision and Review; WEP: Review and Editing.

ACKNOWLEDGEMENT

This research is supported by the RKAT PTNBH Universitas Sebelas Maret Fiscal Year 2024 through the APPLIED SUPERIOR RESEARCH (PUT-UNS) Research scheme with Research Assignment Agreement Number: 194.2/UN27.22/PT.01.03/2024.

REFERENCES

Aghapur, N., Gharbavi, M., Bigdelou, Z., Zand, M., and Johari, B., 2025. Green Synthesis of Silver Nanoparticles Coated with Methotrexate-Conjugated Polyvinyl Alcohol: As Potential Nanosystem for Chemo/Radiotherapy. *Journal of Drug Delivery Science and Technology*, 105, 106643. https://doi.org/10.1016/j.jddst.2025.106643.

Aini, N., Purwono, B., and Tahir, I., 2010. Structure – Antioxidant Activities Relationship Analysis of Isoeugenol, Eugenol, Vanilin and Their Derivatives. *Indonesian Journal of Chemistry*, 7, 61–66. https://doi.org/10.22146/ijc.21714.

Al Ridho, E., Sari, R., and Wahdaningsih, S., 2013. Uji Aktivitas Antioksidan Ekstrak Metanol Buah Lakum (*Cayratia trifolia*) dengan Metode DPPH (2,2-Difenil- 1-Pikrilhidrazill). *Jurnal Mahasiswa Farmasi Fakultas Kedokteran UNTAN*, 1, 1–11.

Amaya-Flórez, A., Serrano-García, J.S., Ruiz-Galindo, J., Arenaza-Corona, A., Cruz-Navarro, J.A., Orjuela, A.L., Alí-Torres, J., Flores-Alamo, M., Cano-Sanchez, P., Reyes-Márquez, V., and Morales-Morales, D., 2024. POCOP-Ni(II) Pincer Compounds Derived from Phloroglucinol. Cytotoxic and Antioxidant Evaluation. *Frontiers in Chemistry*, 12, 1–17. https://doi.org/10.3389/fchem.2024.1483999.

Aminudin, N.I., Ahmad, F., and Taher, M., 2019. Antibacterial and Antioxidant Activities of Extracts from *Calophyllum ferrugineum* and *Calophyllum incrassatum*. *Malaysian Journal of Analytical Sciences*, 23, 637–647. https://doi.org/10.17576/mjas-2019-2304-09.

Aneesa, F., Rajanna, K.C., Arun Kumar, Y., and Arifuddin, M., 2012. Transition Metal Ions as Efficient Catalysts for Facile Ortho-Formylation of Phenols under Vilsmeier–Haack Conditions. *Organic Chemistry International*, 2012, 1–7. https://doi.org/10.1155/2012/289023.

Anggraini, S.D., 2019. Sintesis Diasetilfloroglusinol (DAPG) dan Dimer Diasetilfloroglusinol (DDAPG) serta Uji Aktivitas Antibakteri. *Skripsi*. Universitas Sebelas Maret, Surakarta.

Aparamarta, H.W., Hapsari, S., Ismawan, R., Anggraeni, V., Widjaja, A., Widjaja, T., Ju, Y.-H., and Gunawan, S., 2018. Separation of Xanthone and Vitamin E from *Calophyllum inophyllum* Leaf. *Malaysian Journal of Fundamental* and *Applied Sciences*, 14, 484–489. https://doi.org/10.11113/mjfas.v14n4.933.

Archana, I., and Vijayalakshmi, K., 2018. Antioxidant Potential of Phloroglucinol; An In-Vitro Approach. *International Journal of Pharmaceutical Sciences* and *Research*, 9, 2947–2951.

Bashir, M., Saifullah, M., Riaz, M., Arshad, M., Irfan, A., Iqbal, S., Farooqi, Z.H., and Begum, R., 2023. Schiff Bases Derived from Phloroglucinol Carbonyl Variants and Their Applications-A Review. *Inorganic Chemistry Communications*, 152, 110690. https://doi.org/10.1016/j.inoche.2023.110690.

Biessy, A., and Filion, M., 2021. Phloroglucinol Derivatives in Plant-Beneficial *Pseudomonas spp.*: Biosynthesis, Regulation, and Functions. *Metabolites*, 11, 182. https://doi.org/10.3390/metabo11030182.

Bota, W., Martosupono, M., and Rondonuwu, F.S., 2015. Potensi Senyawa Minyak Sereh Wangi (*Citronella oil*) dari Tumbuhan *Cymbopogon nardus* L. sebagai Agen Antibakteri, *Seminar Nasional dan Teknologi*. 17 November 2015, Fakultas Teknik, Universitas Muhammadiyah Jakarta, 137.

Bridi, H., Meirelles, G. de C., and von Poser, G.L., 2018. Structural Diversity and Biological Activities of Phloroglucinol Derivatives from Hypericum Species. *Phytochemistry*, 155, 203–232. https://doi.org/10.1016/j.phytochem.2018.08.002.

Cahyani, S.D., 2023. Sintesis Asetilfloroglusinol-Ninhidrin dan Uji Aktivitas Antibakteri serta Antioksidan. *Skripsi*. Universitas Sebelas Maret, Surakarta.

Casero, C., Machín, F., Méndez-Álvarez, S., Demo, M., Ravelo, Á.G., Pérez-Hernández, N., Joseph-Nathan, P., and Estévez-Braun, A., 2015. Structure and Antimicrobial Activity of Phloroglucinol Derivatives from *Achyrocline Satureioides*. *Journal of Natural Products*, 78, 93–102. https://doi.org/10.1021/np500735f.

Chahal, M., Dhillon, S., Rani, P., Kumari, G., Aneja, D.K., and Kinger, M., 2023. Unravelling the Synthetic and Therapeutic Aspects of Five, Six and Fused Heterocycles Using Vilsmeier–Haack Reagent. *RSC Advances*, 13, 26604–26629. https://doi.org/10.1039/D3RA04309F.

Chapman, E.E., Langler, R.F., and Crandall, I., 2008. Phloroglucinol Sulfonic Acid Esters as Antimalarial/Anticancer Agents. *Journal of Sulfur Chemistry*, 29, 607–618. https://doi.org/10.1080/17415990802346010.

Chauthe, S.K., Bharate, S.B., Periyasamy, G., Khanna, A., Bhutani, K.K., Mishra, P.D., and Singh, I.P., 2012. One Pot Synthesis and Anticancer Activity of Dimeric Phloroglucinols. *Bioorganic & Medicinal Chemistry Letters*, 22, 2251–2256. https://doi.org/10.1016/j.bmcl.2012.01.089.

Chen, J., Yang, J., Ma, L., Li, J., Shahzad, N., and Kim, C.K., 2020. Structure-Antioxidant Activity Relationship of Methoxy, Phenolic Hydroxyl, and Carboxylic Acid Groups of Phenolic Acids. *Scientific Reports*, 10. https://doi.org/10.1038/s41598-020-59451-z.

Chen, Y., Zheng, W., Song, X., Pan, D., Zhuo, Y., Yang, Z., Wang, Q., Wu, Y., and Gu, J., 2024. Structurally Diverse Phenylpropanoyl Phloroglucinol Derivatives from *Mallotus philippensis* and Their Anti-Bacterial Activities. *Bioorganic Chemistry*, 153, 107918. https://doi.org/10.1016/j.bioorg.2024.107918.

Delfanian, M., Sahari, M.A., Barzegar, M., and Ahmadi Gavlighi, H., 2021. Structure–Antioxidant Activity Relationships of Gallic Acid and Phloroglucinol. *Journal of Food Measurement* and *Characterization*, 15, 5036–5046. https://doi.org/10.1007/s11694-021-01045-y.

Diniyah, N., and Lee, S.-H., 2020. Komposisi Senyawa Fenol dan Potensi Antioksidan dari Kacang-Kacangan: Review. *Jurnal Agroteknologi*, 14, 91. https://doi.org/10.19184/j-agt.v14i01.17965.

Farias, I. V., Faqueti, L.G., Noldin, V.F., Franchi Junior, G., Nowil, A.E., Schuquel, I.T.A., Delle Monache, F., García, P.A., López-Pérez, J.L., San Feliciano, A., Cechinel-Filho, V., and Meyre-Silva, C., 2018. Cytotoxic Phloroglucinol Meroterpenoid from *Eugenia umbelliflora* Fruits. *Phytochemistry Letters*, 27, 187–192. https://doi.org/10.1016/j.phytol.2018.07.004.

Flores, C.Y., Miñán, A.G., Grillo, C.A., Salvarezza, R.C., Vericat, C., and Schilardi, P.L., 2013. Citrate-Capped Silver Nanoparticles Showing Good Bactericidal Effect against Both Planktonic and Sessile Bacteria and a Low Cytotoxicity to Osteoblastic Cells. *ACS Applied Materials & Interfaces*, 5, 3149–3159. https://doi.org/10.1021/am400044e.

García-Eleno, M.A., Padilla-Mata, E., Estudiante-Negrete, F., Pichal-Cerda, F., Hernández-Ortega, S., Toscano, R.A., and Morales-Morales, D., 2015. Single Step, High Yield Synthesis of Para-Hydroxy Functionalized POCOP Ligands and Their Ni(II) Pincer Derivatives. *New Journal of Chemistry*, 39, 3361–3365. https://doi.org/10.1039/c5nj00052a.

Hamiche, S., Bensouici, C., Messaoudi, A., Gali, L., Khelouia, L., Rateb, M.E., Akkal, S., Badis, A., and Hattab, M. El, 2021. Antioxidant and Structure–Activity Relationship of Acylphloroglucinol Derivatives from the Brown Alga Zonaria Tournefortii. *Monatshefte für Chemie - Chemical Monthly*, 152, 431–440. https://doi.org/10.1007/s00706-021-02748-0.

He, X.-Z., Liu, H., Yan, H., Ni, W., Fang, X., and Liu, H.-Y., 2025. Isolation, Characterization, and Anti-MRSA Activity of Formyl-Phloroglucinol-Derivatives from *Eucalyptus robusta* Fruits. *Journal of Molecular Structure*, 1322, 140388. https://doi.org/10.1016/j.molstruc.2024.140388.

Heleno, S.A., Martins, A., Queiroz, M.J.R.P., and Ferreira, I.C.F.R., 2015. Bioactivity of Phenolic Acids: Metabolites versus Parent Compounds: A Review. *Food Chemistry*, 173, 501–513. https://doi.org/10.1016/j.foodchem.2014.10.057.

Henry, G.E., Campbell, M.S., Zelinsky, A.A., Liu, Y., Bowen-Forbes, C.S., Li, L., Nair, M.G., Rowley, D.C., and Seeram, N.P., 2009. Bioactive Acylphloroglucinols from *Hypericum Densiflorum*. *Phytotherapy Research*, 23, 1759–1762. https://doi.org/10.1002/ptr.2845.

Hertiningtyas, C., Kusumaningsih, T., and Firdaus, M., 2020. A Novel Synthesis of 1,1'-(2,4,6-Trihydroxy-1,3-Phenylene)Bis(Ethan-1-One) (DAPG) Using $CuSO_4.5H_2O$ as a Green Catalyst. *AIP Conference Proceedings*. AIP Publishing, 020018. https://doi.org/10.1063/5.0005344.

Hidayah, N., Mustikaningtyas, D., and Bintari, S.H., 2017. Antibacterial Activity of *Sargassum muticum* Simplisia Infusion on the Growth of *Staphylococcus aureus*. *Life Science*, 6, 49–54.

Hiranrat, A., and Mahabusarakam, W., 2008. New Acylphloroglucinols from the Leaves of *Rhodomyrtus tomentosa*. *Tetrahedron*, 64, 11193–11197. https://doi.org/10.1016/j.tet.2008.09.054.

Hossain, T.J., 2024. Methods for Screening and Evaluation of Antimicrobial Activity: A Review of Protocols, Advantages, and Limitations. *European Journal of Microbiology* and *Immunology*, 14, 97–115. https://doi.org/10.1556/1886.2024.00035.

Huang, J., Li, Chuang-Jun, Yang, J., Li, Chuan, Zhang, Y., Liu, K., Yu, Y., Jiang, J., and Zhang, D., 2021. Guajamers A—I, Rearranged Polycyclic Phloroglucinol Meroterpenoids from *Psidium Guajava* Leaves and Their Antibacterial Activity. *Chinese Journal of Chemistry*, 39, 1129–1137. https://doi.org/10.1002/cjoc.202000640.

Jawetz, E., Melnick, J.L., and Adelberg, E.A., 2014. *Medical Microbiology*, twenty sixth ed, Notes and Queries.

Jégou, C., Kervarec, N., Cérantola, S., Bihannic, I., and Stiger-Pouvreau, V., 2015. NMR Use to Quantify Phlorotannins: The Case of *Cystoseira tamariscifolia*, a Phloroglucinol-Producing Brown Macroalga in Brittany (France). *Talanta*, 135, 1–6. https://doi.org/10.1016/j.talanta.2014.11.059.

Kang, S.-M., Heo, S.-J., Kim, K.-N., Lee, S.-H., and Jeon, Y.-J., 2012. Isolation and Identification of New Compound, 2,7″-Phloroglucinol-6,6′-Bieckol from Brown Algae, Ecklonia Cava and Its Antioxidant Effect. *Journal of Functional Foods*, 4, 158–166. https://doi.org/10.1016/j.jff.2011.10.001.

Kang, S.-M., Lee, S.-H., Heo, S.-J., Kim, K.-N., and Jeon, Y.-J., 2011. Evaluation of Antioxidant Properties of a New Compound, Pyrogallol-Phloroglucinol-6,6'-Bieckol Isolated from Brown Algae, *Ecklonia Cava*. *Nutrition Research* and *Practice*, 5, 495–502. https://doi.org/10.4162/nrp.2011.5.6.495.

Kim, R.K., Suh, Y., Yoo, K., Cui, Y., Hwang, E., Kim, H., Kang, J., Kim, M., Lee, Y.Y., and Lee, S., 2015. Phloroglucinol Suppresses Metastatic Ability of Breast Cancer Cells by Inhibition of Epithelial-mesenchymal Cell Transition. *Cancer Science*, 106, 94–101. https://doi.org/10.1111/cas.12562.

Kim, R.K., Uddin, N., Hyun, J.-W., Kim, C., Suh, Y., and Lee, S.-J., 2015. Novel Anticancer Activity of Phloroglucinol against Breast Cancer Stem-like Cells. *Toxicology* and *Applied Pharmacology*, 286, 143–150. https://doi.org/10.1016/j.taap.2015.03.026.

Kong, C.-S., Kim, J.-A., Yoon, N.-Y., and Kim, S.-K., 2009. Induction of Apoptosis by Phloroglucinol Derivative from Ecklonia Cava in MCF-7 Human Breast Cancer Cells. *Food* and *Chemical Toxicology*, 47, 1653–1658. https://doi.org/10.1016/j.fct.2009.04.013.

Kumar, P., Yuvakkumar, R., Vijayakumar, S., and Vaseeharan, B., 2018. Cytotoxicity of Phloroglucinol Engineered Silver (Ag) Nanoparticles against MCF-7 Breast Cancer Cell Lines. *Materials Chemistry* and *Physics*, 220, 402–408. https://doi.org/10.1016/j.matchemphys.2018.08.074.

Kundu, S.K., Patra, A., and Pramanik, A., 2004. Facile Acid-Catalyzed Condensation of Ninhydrin with Enols and Aromatic Compounds and Microwave Enhanced Condensation of Ninhydrin with Hydroxy Aromatic Systems in Solid State. *Indian Journal of Chemistry - Section B Organic* and *Medicinal Chemistry*, 43, 604–611. https://doi.org/10.1002/chin.200428051.

Kusumaningsih, T., Firdaus, M., Artanti, A.N., and Prasetyo, W.E., 2019. Highly Efficient One Pot Synthesis of Triacetylphloroglucinol: An Analogue of Acylphloroglucinol Natural Product. *IOP Conference Series: Materials Science* and *Engineering*, 578, 012057. https://doi.org/10.1088/1757-899X/578/1/012057.

Kusumaningsih, T., Firdaus, M., Wartono, M.W., Artanti, A.N., Handayani, D.S., and Putro, A.E., 2016. Ethyl-2-(3,5-Dihidroxyfenol): Phloroglucinol Derivatives as Potential Anticancer Material. *IOP Conference Series: Materials Science* and *Engineering*, 107, 012059. https://doi.org/10.1088/1757-899X/107/1/012059.

Kusumaningsih, T., Prasetyo, W.E., and Firdaus, M., 2020. A Greatly Improved Procedure for the Synthesis of an Antibiotic-Drug Candidate 2,4-Diacetylphloroglucinol over Silica Sulphuric Acid Catalyst: Multivariate Optimisation and Environmental Assessment Protocol Comparison by Metrics. *RSC Advances*, 10, 31824–31837. https://doi.org/10.1039/D0RA05424K.

Kusumaningsih, T., Prasetyo, W.E., Istiqomah, A., Firdaus, M., and Wibowo, F.R., 2023. Sustainable Synthesis of Silver Nanoparticles with Enhanced Anticancer, Antibacterial, and Antioxidant Properties Mediated by Dimeric 2,4-Diacetyl Phloroglucinol: Experimental and Computational Insights. *Surfaces* and *Interfaces*, 36, 102545. https://doi.org/10.1016/j.surfin.2022.102545.

Lee, D.S., Cho, Y.S., and Je, J.Y., 2013. Antioxidant and Antibacterial Activities of Chitosan-Phloroglucinol Conjugate. *Fisheries* and *Aquatic Sciences*, 16, 229–235. https://doi.org/10.5657/FAS.2013.0229.

Lee, H.B., Kim, J.C., and Lee, S.M., 2009. Antibacterial Activity of Two Phloroglucinols, Flavaspidic Acids AB and PB, from *Dryopteris crassirhizoma*. *Archives of Pharmacal Research*, 32, 655–659. https://doi.org/10.1007/s12272-009-1502-9.

Lee, S.-M., Na, M.-K., An, R.-B., Min, B.-S., and Lee, H.-K., 2003. Antioxidant Activity of Two Phloroglucinol Derivatives from *Dryopteris crassirhizoma*. *Biological* and *Pharmaceutical Bulletin*, 26, 1354–1356. https://doi.org/10.1248/bpb.26.1354.

Li, Y., Qian, Z.-J., Ryu, B., Lee, S.-H., Kim, M.-M., and Kim, S.-K., 2009. Chemical Components and Its Antioxidant Properties in Vitro: An Edible Marine Brown Alga, Ecklonia Cava. *Bioorganic & Medicinal Chemistry*, 17, 1963–1973. https://doi.org/10.1016/j.bmc.2009.01.031.

Liswandari, M.S., 2018. Uji Aktivitas Antibakteri Alga Hijau (*Ulva sp.*) dari Pantai Sorido Biak terhadap Bakteri *Escherichia coli* dan *Staphylococcus aureus*. *Jurnal Farmasi Medica/Pharmacy Medical Journal (PMJ)*, 1, 9–15. https://doi.org/10.35799/pmj.1.1.2018.19646.

Mahapatra, A., Prasad, T., and Sharma, T., 2021. Pyrimidine: A Review on Anticancer Activity with Key Emphasis on SAR. *Future Journal of Pharmaceutical Sciences*, 7, 123. https://doi.org/10.1186/s43094-021-00274-8.

Marinova, G., and Batchvarov, V., 2011. Evaluation of the Methods for Determination of the Free Radical Scavenging Activity by DPPH. *Bulgarian Journal of Agricultural Science*, 17, 11–24.

McMurry, J., 2008. *Organic Chemistry*, seventh ed. Thomson Learning Inc, United States of Amerika.

Mo, Q.-H., Yan, M.-Q., Zhou, X.-L., Luo, Q., Huang, X.-S., and Liang, C.-Q., 2021. Phloroglucinol Derivatives Rhotomensones A-G from *Rhodomyrtus tomentosa*. *Phytochemistry*, 190, 112890. https://doi.org/10.1016/j.phytochem.2021.112890.

Mohamed, E.A., Ismail, N.S.M., Hagras, M., and Refaat, H., 2021. Medicinal Attributes of Pyridine Scaffold as Anticancer Targeting Agents. *Future Journal of Pharmaceutical Sciences*, 7. https://doi.org/10.1186/s43094-020-00165-4.

Mondal, M., T, P.L., Krishna, R., and Sakthivel, N., 2017. Molecular Interaction between Human Serum Albumin (HSA) and Phloroglucinol Derivative That Shows Selective Anti-Proliferative Potential. *Journal of Luminescence*, 192, 990–998. https://doi.org/10.1016/j.jlumin.2017.08.007.

Morkunas, M., Dube, L., Götz, F., and Maier, M.E., 2013. Synthesis of the Acylphloroglucinols Rhodomyrtone and Rhodomyrtosone B. *Tetrahedron*, 69, 8559–8563. https://doi.org/10.1016/j.tet.2013.07.091.

Nandiyanto, A.B.D., Oktiani, R., and Ragadhita, R., 2019. How to Read and Intrepret FTIR Spectroscope of Organic Material. *Indonesian Journal of Science & Technology*, 4, 97–118.

Nagel, K., Schneemann, I., Kajahn, I., Labes, A., Wiese, J., and Imhoff, J., 2012. Beneficial Effects of 2,4-Diacetylphloroglucinol- Producing Pseudomonads on the Marine Alga *Saccharina latissima*. *Aquatic Microbial Ecology*, 67, 239–249. https://doi.org/10.3354/ame01595.

Nayak, Y.N., Nayak, S., Nadaf, Y.F., Shetty, N.S., and Gaonkar, S.L., 2019. Zeolite Catalyzed Friedel-Crafts Reactions: A Review. *Letters in Organic Chemistry*, 17, 491–506. https://doi.org/10.2174/1570178616666190807101012.

Nguyen, A. Van, Vu, A.T.N., Bazan, L. V., Galeev, R.T., Utenyshev, A.N., Markova, E.B., Le, V.T., and Kovalchukova, O. V., 2022. Synthesis, Characterization, and Sorption Activity of Novel Azo-Colorants Derived from Phloroglucinol and Antipyrine and Their Metal Complexes. *RSC Advances*, 12, 888–898. https://doi.org/10.1039/D1RA07254D.

Noviany, N., Amrulloh, M.H., Mohamad Rafi, M.R., Bambang Irawan, B.I., Wisnu Ananta Kusuma, W.A.K., Sutopo Hadi, S.H., Supriyanto, R., Risa Nofiani, R.N., Hussin, M.H., and Suripto Dwi Yuwono, S.D.Y., 2023. FTIR-Based Metabolomics for Characterization of Antioxidant Activity of Different Parts of *Sesbania grandiflora* Plant. *Sains Malaysiana*, 52, 165–174. https://doi.org/10.17576/jsm-2023-5201-13.

Oziminski, W.P., and Wójtowicz, A., 2020. New Theoretical Insights on Tautomerism of Hyperforin—a Prenylated Phloroglucinol Derivative Which May Be Responsible for St. John's Wort (*Hypericum perforatum*) Antidepressant Activity. *Structural Chemistry*, 31, 657–666. https://doi.org/10.1007/s11224-019-01434-6.

Peron, G., López, A.M., Cabada-Aquirre, P., Garay Buenrosto, K.D., Ostos Mendoza, K.C., Mahady, G.B., Seidel, V., Sytar, O., Koirala, N., Gurung, R., Acharya, Z., Adhikari, S., Sureda, A., Martorell, M., and Sharifi-Rad, J., 2024. Antiviral and Antibacterial Properties of Phloroglucinols: A Review on Naturally Occurring and (Semi)Synthetic Derivatives with Potential Therapeutic Interest. *Critical Reviews in Biotechnology*, 44, 319–336. https://doi.org/10.1080/07388551.2022.2160695.

Phongpaichit, S., Nikom, J., Rungjindamai, N., Sakayaroj, J., Hutadilok-Towatana, N., Rukachaisirikul, V., and Kirtikara, K., 2007. Biological Activities of Extracts from Endophytic Fungi Isolated from *Garcinia* Plants. *FEMS Immunology & Medical Microbiology*, 51, 517–525. https://doi.org/10.1111/j.1574-695X.2007.00331.x.

Prabawati, S.Y., 2016. Synthesis of 1,4-Bis [(1-Hydroxy-4-T-Butyl-Phenyl) Methyl]Piperazine as an Antioxidant. *Molekul*, 11, 220. https://doi.org/10.20884/1.jm.2016.11.2.244.

Prasetyo, W.E., Kusumaningsih, T., and Firdaus, M., 2019. Highly Efficient and Green Synthesis of Diacylphloroglucinol over Treated Natural Zeolite Mordenite and the Optimization Using Response Surface Method (RSM). *Synthetic Communications*, 49, 3352–3372. https://doi.org/10.1080/00397911.2019.1666282.

Prasetyo, W.E., Kusumaningsih, T., Firdaus, M., Marliana, S.D., Suryanti, V., Artanti, A.N., Apriana, I., and Anggraini, S.D., 2022. Diacylphloroglucinol Derivatives as Antioxidant Agents: Green Synthesis, Optimisation, In Vitro, and In Silico Evaluation. *Natural Product Research*, 36. https://doi.org/10.1080/14786419.2021.1889542.

Prasetyo, W.E., Kusumaningsih, T., Triadmojo, B., Anggraini, S.D., Marliyana, S.D., and Firdaus, M., 2023. Investigation of the Dual Role of Acyl Phloroglucinols as a New Hope for Antibacterial and Anti-SARS-

CoV-2 Agents Employing Integrated In Vitro and Multi-Phase In Silico Approaches. *Journal of Biomolecular Structure* and *Dynamics*, 41. https://doi.org/10.1080/07391102.2023.2186712.

Rahmaniar, W., 2023. Sintesis 4b,7,9,9b-Tetrahidroksi-8-Isobutiril-4bh-Indeno[1,2-B]Benzofuran-10(9bh)-One serta Uji Aktivitas Antibakteri dan Antioksidan. *Skripsi*. Universitas Sebelas Maret, Surakarta.

Rayan, A., Raiyn, J., and Falah, M., 2017. Nature Is the Best Source of Anticancer Drugs: Indexing Natural Products for Their Anticancer Bioactivity. *PLOS ONE*, 12, e0187925. https://doi.org/10.1371/journal.pone.0187925.

Reber, K.P., Sivey, J.D., Vollmuth, M., and Gujarati, P.D., 2022. Synthesis of ^{13} C-labeled Parabens from Isotopically Enriched Phenols Using the Houben–Hoesch Reaction. *Journal of Labelled Compounds* and *Radiopharmaceuticals*, 65, 254–263. https://doi.org/10.1002/jlcr.3992.

Rohdiana, D., Arief, D.Z., and Budiman, A., 2013. Aktivitas Penghambatan Pertumbuhan Bakteri *Escherichia coli* oleh Berbagai Jenis Teh dan Seduhannya. *Jurnal Penelitian Teh dan Kina*, 16, 37–44.

Ruiz-Torres, V., Encinar, J., Herranz-López, M., Pérez-Sánchez, A., Galiano, V., Barrajón-Catalán, E., and Micol, V., 2017. An Updated Review on Marine Anticancer Compounds: The Use of Virtual Screening for the Discovery of Small-Molecule Cancer Drugs. *Molecules*, 22, 1037. https://doi.org/10.3390/molecules22071037.

Sanjai, C., Hakkimane, S.S., Guru, B.R., and Gaonkar, S.L., 2024. A Comprehensive Review on Anticancer Evaluation Techniques. *Bioorganic Chemistry*, 142, 106973. https://doi.org/10.1016/j.bioorg.2023.106973.

Sarvari, M.H., and Sharghi, H., 2004. Reactions on a Solid Surface. A Simple, Economical and Efficient Friedel−Crafts Acylation Reaction over Zinc Oxide (ZnO) as a New Catalyst. *The Journal of Organic Chemistry*, 69, 6953–6956. https://doi.org/10.1021/jo0494477.

Sato, Y., Yato, M., Ohwada, T., Saito, S., and Shudo, K., 1995. Involvement of Dicationic Species as the Reactive Intermediates in Gattermann, Houben-Hoesch, and Friedel—Crafts Reactions of Nonactivated Benzenes. *Journal of the American Chemical Society*, 117, 3037–3043. https://doi.org/10.1021/ja00116a009.

Shamsudin, N.F., Ahmed, Q.U., Mahmood, S., Ali Shah, S.A., Khatib, A., Mukhtar, S., Alsharif, M.A., Parveen, H., and Zakaria, Z.A., 2022. Antibacterial Effects of Flavonoids and Their Structure-Activity Relationship Study: A Comparative Interpretation. *Molecules*, 27, 1149. https://doi.org/10.3390/molecules27041149.

Shanmugam, L., Venkatasubbu, G.D., and Jayaraman, M., 2024. Hyaluronan-Based Nano-Formulation with Mesoporous Silica Enhances the Anticancer Efficacy of Phloroglucinol against Gastrointestinal Cancers. *International Journal of Biological Macromolecules*, 265. https://doi.org/10.1016/j.ijbiomac.2024.130856.

Sholihah, M., 2023. Sintesis Monoisovalerilfloroglusinol-Ninhidrin serta Uji Aktivitas Antibakteri dan Antioksidan. *Thesis*. Universitas Sebelas Maret, Surakarta.

Shin, H.-C., Kim, Y., Choi, J., Kang, H.B., Han, S.-Y., Park, K., and Hwang, H.J., 2022. Regioselective Synthesis of 6-O-Acetyl Dieckol and Its Selective Cytotoxicity against Non-Small-Cell Lung Cancer Cells. *Marine Drugs*, 20, 683. https://doi.org/10.3390/md20110683.

Singh, I.P., and Bharate, S.B., 2006. Phloroglucinol Compounds of Natural Origin. *Natural Product Reports*, 23, 558–591. https://doi.org/10.1039/b600518g.

Singh, I.P., Sidana, J., Bansal, P., and Foley, W.J., 2009. Phloroglucinol Compounds of Therapeutic Interest: Global Patent and Technology Status. *Expert Opinion on Therapeutic Patents*, 19, 847–866. https://doi.org/10.1517/13543770902916614.

Soliman, F.M., Fathy, M.M., Salama, M.M., Al-Abd, A.M., Saber, F.R., and El-Halawany, A.M., 2014. Cytotoxic Activity of Acyl Phloroglucinols Isolated from the Leaves of *Eucalyptus cinerea* F. Muell. Ex Benth. Cultivated in Egypt. *Scientific Reports*, 4, 5410. https://doi.org/10.1038/srep05410.

Sun, Q., Schmidt, S., Tremmel, M., Heilmann, J., and König, B., 2014. Synthesis of Natural-like Acylphloroglucinols with Anti-Proliferative, Anti-Oxidative and Tube-Formation Inhibitory Activity. *European Journal of Medicinal Chemistry*, 85, 621–628. https://doi.org/10.1016/j.ejmech.2014.08.017.

Surahmaida, S., and Lestari, K.A.P., 2019. Uji Aktivitas Kombucha Teh dan Kopi sebagai Antibakteri Bakteri Gram Positif dan Bakteri Gram Negatif. *Journal Pharmasci (Journal of Pharmacy* and *Science)*, 4, 61–65. https://doi.org/10.53342/pharmasci.v4i2.135.

Suryani, R., Rizal, W.A., Pratiwi, D., and Prasetyo, D.J., 2020. Karakteristik dan Aktivitas Antibakteri Asap Cair dari Biomassa Kayu Putih (*Melaleuca leucadendra*) dan Kayu Jati (*Tectona grandis*). *Jurnal Teknologi Pertanian*, 21, 106–117. https://doi.org/10.21776/ub.jtp.2020.021.02.4.

Syed, B., Nagendra Prasad, M.N., Mohan Kumar, K., and Satish, S., 2018. Bioconjugated Nano-Bactericidal Complex for Potent Activity against Human and Phytopathogens with Concern of Global Drug Resistant Crisis. *Science of The Total Environment*, 637–638, 274–281. https://doi.org/10.1016/j.scitotenv.2018.04.405.

Tahara, A.R., 2023. Sintesis 4b,7,9,9b-Tetrahidroksi-4bh-Indeno[1,2-B] Benzofuran-10(9bh)-On serta Uji Aktivitasnya sebagai Antioksidan dan Antibakteri. Skripsi. Universitas Sebelas Maret, Surakarta.

Tan, H., Liu, H., Zhao, L., Yuan, Y., Li, B., Jiang, Y., Gong, L., and Qiu, S., 2017. Structure-Activity Relationships and Optimization of Acyclic Acylphloroglucinol Analogues as Novel Antimicrobial Agents. *European Journal of Medicinal Chemistry*, 125, 492–499. https://doi.org/10.1016/j.ejmech.2016.09.054.

Tan, J.B.L., and Lim, Y.Y., 2015. Critical Analysis of Current Methods for Assessing the In Vitro Antioxidant and Antibacterial Activity of Plant Extracts. *Food Chemistry*, 172, 814–882. https://doi.org/10.1016/j.foodchem.2014.09.141.

Tang, L., Fu, L., Lu, C., Hou, X., Shan, W., and Zhan, Z., 2017. New Cytotoxic Phloroglucinol Derivatives from *Agrimonia pilosa*. *Fitoterapia*, 118, 69–72. https://doi.org/10.1016/j.fitote.2017.02.010.

Tchangoue, Y.A.N., Tchamgoue, J., Lunga, P.K., Knepper, J., Paltinean, R., Ibrom, K., Crișan, G., Kouam, S.F., Ali, M.S., and Schulz, S., 2020. Antibacterial Phloroglucinols Derivatives from the Leaves of *Mallotus oppositifolius* (Geisler) Müll. Arg. (Euphorbiaceae). *Fitoterapia*, 142, 104527. https://doi.org/10.1016/j.fitote.2020.104527.

Triadmojo, N., 2021. Uji Aktivitas Antibakteri dan Antioksidan Senyawa Monoasilfloroglusinol. *Skripsi*. Universitas Sebelas Maret, Surakarta.

Tristantini, D., Ismawati, A., Tegar Pradana, B., and Jonathan, G.J., 2016. Pengujian Aktivitas Antioksidan Menggunakan Metode DPPH pada Daun Tanjung (*Mimusops elengi* L), *Prosiding Seminar Nasional Teknik Kimia "Kejuangan" Pengembangan Teknologi Kimia untuk Pengolahan Sumber Daya Alam Indonesia*, 17 March 2016, Fakultas Teknologi Industri UPN Veteran Yogyakarta, Yogyakarta, Indonesia.

Van Nguyen, A., Ngoc Vu, A.T., Utenyshev, A.N., and Kovalchukova, O. V., 2021. Novel Products of Nitrosation of a Series of Trihydroxybenzene Derivatives and Their Complexation with Cu(II), Cd(II) and Fe(III): Synthesis, Characterization, and Theoretical Modeling. *ChemistrySelect*, 6, 3461–3467. https://doi.org/10.1002/slct.202100227.

Wang, L., He, J., Feng, H., Li, Q., Song, M., Gou, H., He, Y., and Zhu, K., 2025. Antifungal Effects of the Phloroglucinol Derivative DPPG Against Pathogenic *Aspergillus fumigatus*. *Antibiotics*, 14. https://doi.org/10.3390/antibiotics14050499.

Wang, Shuo, Shao, Y., Tian, L., Li, L., Wang, Shuqi, Wang, X., Shen, T., and Ren, D., 2024. Two Rearranged Acylphloroglucinols with Moderate Neuroprotective Effects from *Hypericum ascyron* Linn. *Fitoterapia*, 174, 105852. https://doi.org/10.1016/j.fitote.2024.105852.

Weng, X.C., and Huang, Y., 2014. Relationship Structure-Antioxidant Activity of Hindered Phenolic Compounds. *Grasas y Aceites*, 65. https://doi.org/10.3989/gya.0225141.

Woo, J.Y., and Je, J.Y., 2013. Antioxidant and Tyrosinase Inhibitory Activities of a Novel Chitosan-Phloroglucinol Conjugate. *International Journal of Food Science* and *Technology*, 48, 1172–1178. https://doi.org/10.1111/ijfs.12071.

Xie, Y., Yang, W., Tang, F., Chen, X., and Ren, L., 2014. Antibacterial Activities of Flavonoids: Structure-Activity Relationship and Mechanism. *Current Medicinal Chemistry*, 22, 132–149. https://doi.org/10.2174/09298673216661409161134443.

Xu, W., Zou, X., Zha, Y., Zhang, J., Bian, H., and Shen, Z., 2023. Novel Bis-Artemisinin-Phloroglucinol Hybrid Molecules with Dual Anticancer and Immunomodulatory Activities: Synthesis and Evaluation. *Bioorganic Chemistry*, 139. https://doi.org/10.1016/j.bioorg.2023.106705.

Yan, P., Lai, Q., Li, M., Jin, X., Wie, G., Chen, W., and Ye, L., 2021. New Anticancer Agents: Design, Synthesis, Biological Activity, and Molecular Docking of Bicyclic Phloroglucinol Derivatives. *ChemistrySelect*, 6, 1453–1457. https://doi.org/10.1002/slct.202004442.

Yang, J., Chen, J., Hao, Y., and Liu, Y., 2021. Identification of the DPPH Radical Scavenging Reaction Adducts of Ferulic Acid and Sinapic Acid and Their Structure-Antioxidant Activity Relationship. *LWT*, 146, 111411. https://doi.org/10.1016/j.lwt.2021.111411.

Yang, X., Gao, X., Ou, J., Chen, G., and Ye, L., 2024. Antimicrobial Activity and Mechanism of Anti-MRSA of Phloroglucinol Derivatives. *DARU, Journal of Pharmaceutical Sciences*, 32, 177–187. https://doi.org/10.1007/s40199-024-00503-4.

Yarley, O.P.N., Kojo, A.B., Zhou, C., Yu, X., Gideon, A., Kwadwo, H.H., and Richard, O., 2021. Reviews on Mechanisms of In Vitro Antioxidant, Antibacterial and Anticancer Activities of Water-Soluble Plant Polysaccharides. *International Journal of Biological Macromolecules*, 183, 2262–2271. https://doi.org/10.1016/j.ijbiomac.2021.05.181.

Zhang, F., Lai, Q., Lai, W., Li, M., Jin, X., and Ye, L., 2022. Phloroglucinol Derivatives as Anti-Tumor Agents: Synthesis, Biological Activity Evaluation and Molecular Docking Studies. *Medicinal Chemistry Research*, 31, 165–176. https://doi.org/10.1007/s00044-021-02828-0.